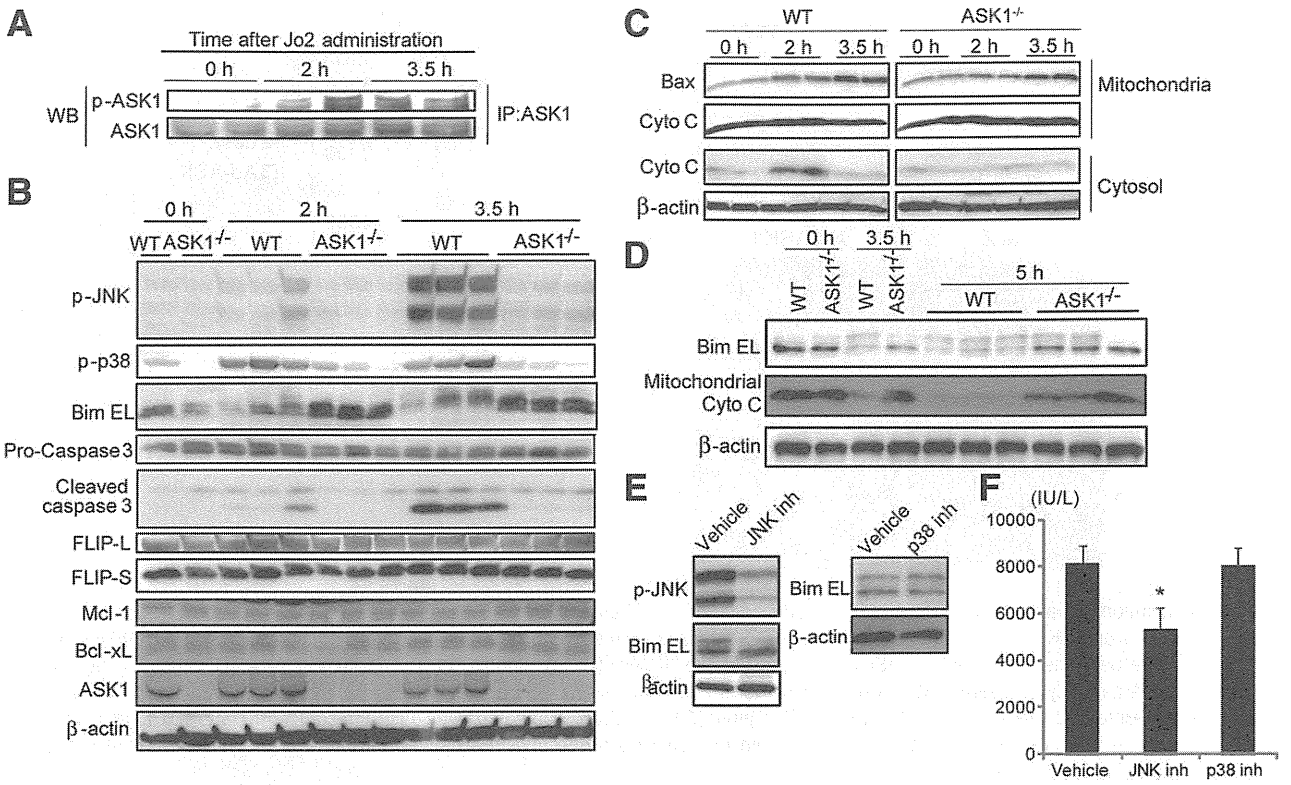

Fig. 5. Analysis of the Fas-signaling pathway. (A) ASK1 activation in WT mouse liver after Jo2 injection. Total liver lysates were immunoprecipitated with ASK1 antibody and analyzed for ASK1 activation by immunoblotting with antibody specific for phospho-ASK1. (B) Western blot analysis of the indicated proteins in WT and ASK1$^{-/-}$ mouse liver. (C) Western blot analysis of Bax and cytochrome *c* in the cytosolic and mitochondrial fractions of WT and ASK1$^{-/-}$ mouse liver. (D) Western blot analysis of BimEL in total liver lysates and of cytochrome *c* in mitochondrial liver fractions from WT and ASK1$^{-/-}$ mice 5 hours after Jo2 administration. (E) Effect of JNK inhibitor and p38 inhibitor on Fas-induced BimEL phosphorylation. (F) Bar graph shows serum ALT levels 5 hours after Jo2 administration to mice pretreated with vehicle, JNK inhibitor, or p38 inhibitor. Data are expressed as means ± SEM (n = 5 per group). *$P < 0.05$, compared with vehicle-treated mice.

derived bone marrow cells showed similar extents of liver injury after Jo2 injection (Fig. 4E,F). These results suggest that ASK1 is involved in Fas-mediated direct hepatocyte apoptosis.

ASK1 Is Required for Activation of the JNK-Bim Pathway in Fas-Induced Apoptotic Signaling. We observed ASK1 phosphorylation after Jo2 administration in WT mouse liver, suggesting that ASK1 was activated in Fas signaling *in vivo* (Fig. 5A). Expression levels of antiapoptotic proteins which have been reported to be implicated in Fas-induced liver injury were not affected by the absence of ASK1 (Fig. 5B). On the other hand, Jo2-induced JNK, p38, and caspase-3 activations were significantly attenuated in ASK1$^{-/-}$ mice compared with WT mice (Fig. 5B).

Bim is phosphorylated by JNK and subsequently cleaved by caspase-3, and becomes a hyperactive inducer of cytochrome *c* release, leading a positive amplification loop in apoptosis.[24,25] In western blot analysis of liver proteins, Jo2 injection induced slower migration of the BimEL band in WT mice, whereas the change in BimEL migration was significantly attenuated in ASK1$^{-/-}$ mice, as also seen in HCC tissues (Fig. 5B). Additionally, we analyzed the activation of the mitochondrial apoptotic pathway, which is essential for Fas-induced apoptosis of hepatocytes (so-called type II cells). The mitochondrial Bax translocation was slightly lower and the cytosolic release of cytochrome *c* was significantly reduced in ASK1$^{-/-}$ mice compared with WT mice at 2 and 3.5 hours after Jo2 administration (Fig. 5C). At 5 hours after Jo2 administration, marked phosphorylation and subsequent degradation of BimEL and reduction of the cytochrome *c* level in the mitochondrial fraction were seen in WT mice, whereas these changes were significantly suppressed in ASK1$^{-/-}$ mice (Fig. 5D). As reported,[19] administration of a JNK inhibitor reduced Jo2-induced BimEL phosphorylation and serum ALT elevation. However, administration of a p38 inhibitor had no detectable effect on BimEL phosphorylation or liver injury (Fig. 5E,F). These results suggest that ASK1 plays an important role in Fas-induced activation of the JNK–Bim–mitochondrial apoptotic pathway.

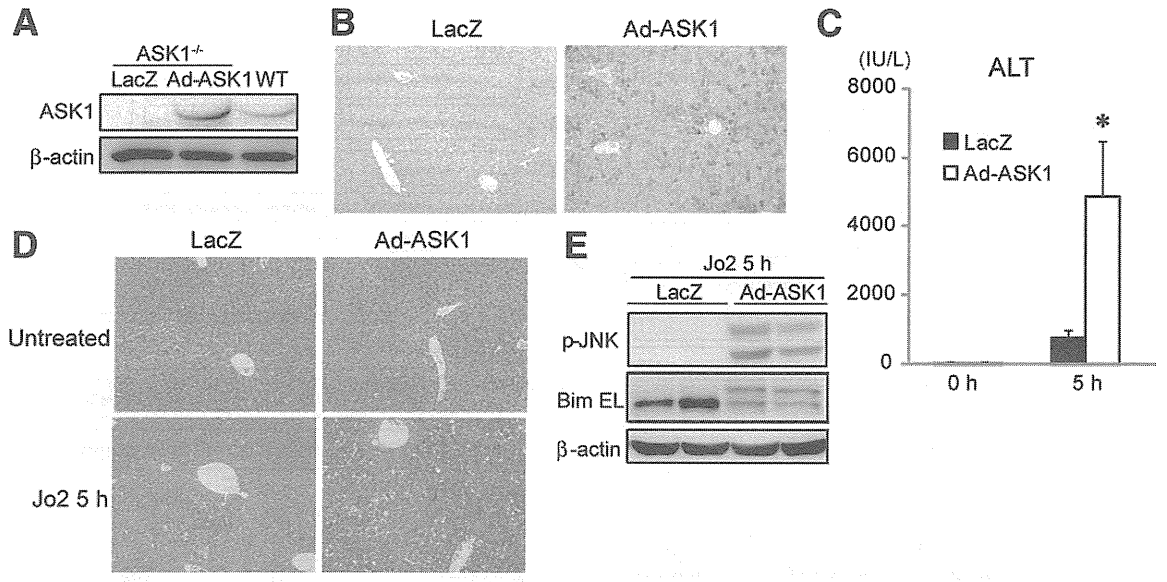

Fig. 6. Restoration of Fas sensitivity in ASK1-reintroduced ASK1$^{-/-}$ mouse liver. (A) Successful adenovirus-mediated expression of ASK1 in ASK1$^{-/-}$ mouse liver. ASK1$^{-/-}$ mice were tail-vein-injected with adenoviruses encoding β-galactosidase (LacZ) or ASK1 (Ad-ASK1). Anti-ASK1 immunoblots were performed to determine ASK1 expression in liver tissue. (B) Immunohistochemical analysis of ASK1 gene transduction in the liver using anti-HA antibody. (C) Serum ALT levels at basal level and 5 hours after Jo2 administration in ASK1$^{-/-}$ mice infected with LacZ or Ad-ASK1. Data are expressed as means ± SEM (n = 3 per group). *$P < 0.05$, compared with mice infected with LacZ. (D) Liver histology with H&E staining of pre- and posttreatment sections. (E) Western blot analysis of the phosphorylation of JNK and BimEL in the liver at 5 hours after Jo2 administration.

Next, to examine whether ASK1 may be involved in a Fas-induced mitochondria-independent apoptotic pathway, we used primary thymocytes, which are independent of mitochondria for Fas-induced apoptosis (so-called type I cells). Fas-induced activation of JNK and p38 was reduced in ASK1$^{-/-}$ thymocytes, whereas caspase-3 activation and cell viability were comparable between WT and ASK1$^{-/-}$ thymocytes (Supporting Fig. 1A,B), suggesting that ASK1 is not required for the mitochondria-independent apoptotic pathway.

Recently, Fas signaling was reported to play a role in not only cancer cell apoptosis, but also cancer cell proliferation.[26] JNK has also been shown to be one of the main mediators of Fas-mediated proliferative signals. To investigate whether ASK1 participated in Fas-mediated hepatocyte proliferation, we injected Jo2 to WT and ASK1$^{-/-}$ mice after partial hepatectomy, which is known to convert Fas signaling from apoptotic to proliferative.[27] As reported,[26,27] Jo2 injection after partial hepatectomy induced JNK phosphorylation and accelerated hepatocyte proliferation without liver injury (Supporting Fig. 2A,B). Although liver regeneration after partial hepatectomy and Jo2-induced JNK phosphorylation were slightly impaired in ASK1$^{-/-}$ mice (especially the upper band corresponding to JNK2), there was no significant difference in Jo2-mediated acceleration of hepatocyte proliferation (Supporting Fig. 2A,B). Thus, ASK1 seemed to regulate the apoptotic, but not proliferative, function of JNK in Fas signaling.

Restoration of Fas Sensitivity in ASK1-Reintroduced ASK1$^{-/-}$ Mouse Liver. To further confirm the involvement of ASK1 in Fas-induced hepatocyte apoptosis, we examined whether the reintroduction of ASK1 to ASK1$^{-/-}$ mouse liver restored sensitivity to Fas. We injected an adenoviral vector encoding either Ad-ASK1 or LacZ into the tail vein of ASK1$^{-/-}$ mice. ASK1 protein was successfully expressed in ASK1$^{-/-}$ mouse liver, as much as that in WT mouse liver, at 48 hours after Ad-ASK1 injection (Fig. 6A). Immunohistochemical analysis using anti-HA antibody revealed that ≈70%-80% of hepatocytes were transduced with the ASK1 gene (Fig. 6B). The reintroduction of ASK1 did not affect the serum ALT level or liver histology. These mice were injected intraperitoneally with Jo2 5 hours later; only mild serum ALT elevation and histological liver damage were found in LacZ-injected mice, whereas Ad-ASK1-injected mice revealed marked serum ALT elevation and severe histological damage (Fig. 6C,D). Furthermore, reintroduction of ASK1 restored Jo2-induced phosphorylation of JNK and BimEL in the liver (Fig. 6E).

Role of ASK1 in TNF-α-Induced Hepatocyte Apoptosis. To examine whether ASK1 is required for TNF-α-induced apoptosis of hepatocytes *in vivo*, we used an LPS/GalN liver injury model that depends on

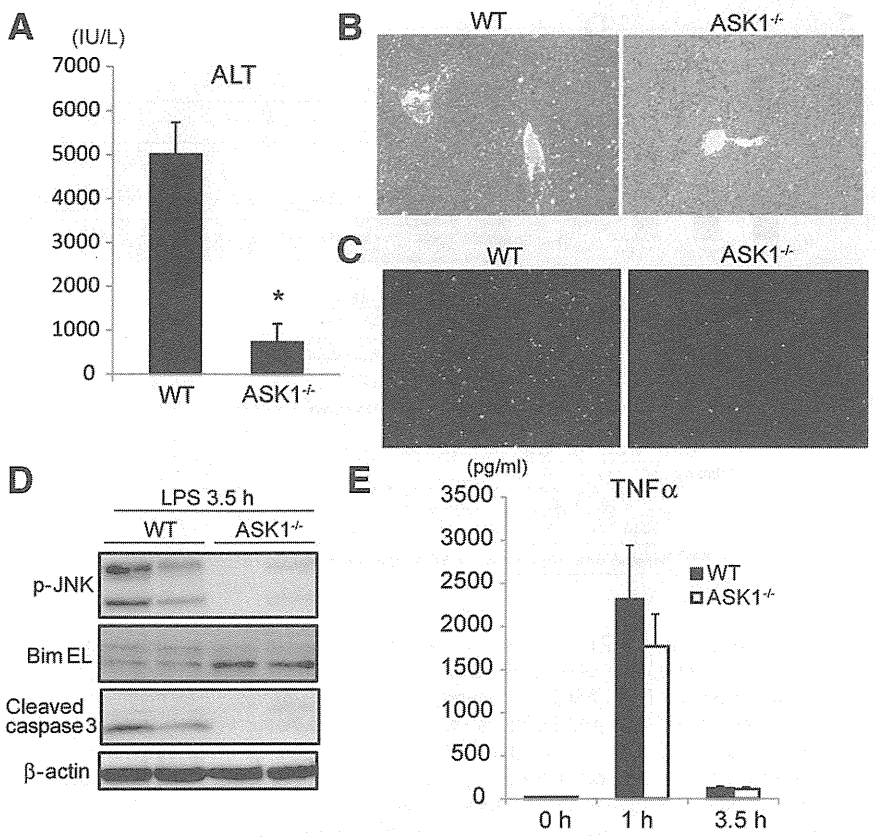

Fig. 7. Involvement of ASK1 in TNF-α-mediated hepatocyte apoptosis. (A) Serum ALT levels 6 hours after the injection of WT and ASK1$^{-/-}$ mice with LPS (20 μg/kg) and GalN (1,000 mg/kg). Data are expressed as means ± SEM (n = 3 per group). *P < 0.05, compared with WT mice. (B) H&E-stained sections of livers obtained 6 hours posttreatment. (C) TUNEL-stained sections of livers obtained 6 hours posttreatment. (D) Western blot analysis of caspase-3, JNK, and Bim activation in WT and ASK1$^{-/-}$ mouse liver obtained 3.5 hours after LPS/GalN administration. (E) Serum TNF-α levels after LPS/GalN administration. Data are expressed as means ± SEM (n = 3 per group).

TNF-α-induced apoptosis.[28] At 6 hours after LPS/GalN administration, WT mice exhibited marked ALT elevation, severe histological liver damage, and hepatocyte apoptosis, whereas these changes were significantly attenuated in ASK1$^{-/-}$ mice (Fig. 7A-C). As expected, LPS/GalN-induced phosphorylation of JNK and BimEL and cleavage of caspase-3 were significantly attenuated in ASK1$^{-/-}$ mice, as well as in Fas-induced liver injury (Fig. 7D). On the other hand, WT and ASK1$^{-/-}$ mice exhibited no significant difference in serum TNF-α levels (Fig. 7E). These findings provide further support for the hypothesis that ASK1 is required for death receptor-mediated hepatocyte apoptosis by way of the JNK–Bim-mediated mitochondrial apoptotic pathway. Furthermore, ASK1 silencing by siRNA attenuated TNF-α-induced sustained JNK and p38 activation, BimEL cleavage, and apoptosis in the HCC cell line HuH7 (Supporting Fig. 3A,B). Thus, resistance to death signaling may be a predominant cause of accelerated hepatocarcinogenesis in ASK1$^{-/-}$ mice.

Involvement of the ASK1-p38 Pathway in DNA Damage Response. Because DEN-induced acute phase reaction in the liver is known to be associated with future HCC development, we assessed the involvement of ASK1 in this phase.[29] Although the DEN-induced activation of JNK was slightly attenuated in ASK1$^{-/-}$ mouse livers, the increases in serum ALT levels were statistically similar in the WT and ASK1$^{-/-}$ mice (Fig. 8A, Supporting Fig. 4A). Bromodeoxyuridine labeling revealed that the numbers of compensatory proliferating hepatocytes in WT and ASK1$^{-/-}$ mice were similar after DEN administration (Supporting Fig. 4B). Furthermore, the level of DEN-induced p53 activation was similar in both groups (Fig. 8A). These findings suggest that DEN induces a similar extent of hepatocyte death, DNA damage, and compensatory proliferation in WT and ASK1$^{-/-}$ mice.

On the other hand, p38 activation was significantly attenuated in the ASK1$^{-/-}$ mouse livers (Fig. 8A), and p38 has been reported to play an important role in DNA damage responses, such as cellular senescence, by inducing cyclin-dependent kinase inhibitors through p53-dependent and -independent mechanisms.[30] Thus, we next compared induction of cyclin-dependent kinase inhibitors after DEN administration between WT and ASK1$^{-/-}$ mouse livers. As shown in Fig. 8B, p16 and p21 were slightly and remarkably induced after DEN administration, respectively, and p21 induction was significantly attenuated in ASK1$^{-/-}$ mouse livers. Because the p38 inhibitor, but not the JNK inhibitor, suppressed DEN-induced p21 up-regulation (Fig. 8C), we considered that the ASK1-p38 pathway may be involved in DNA damage-induced

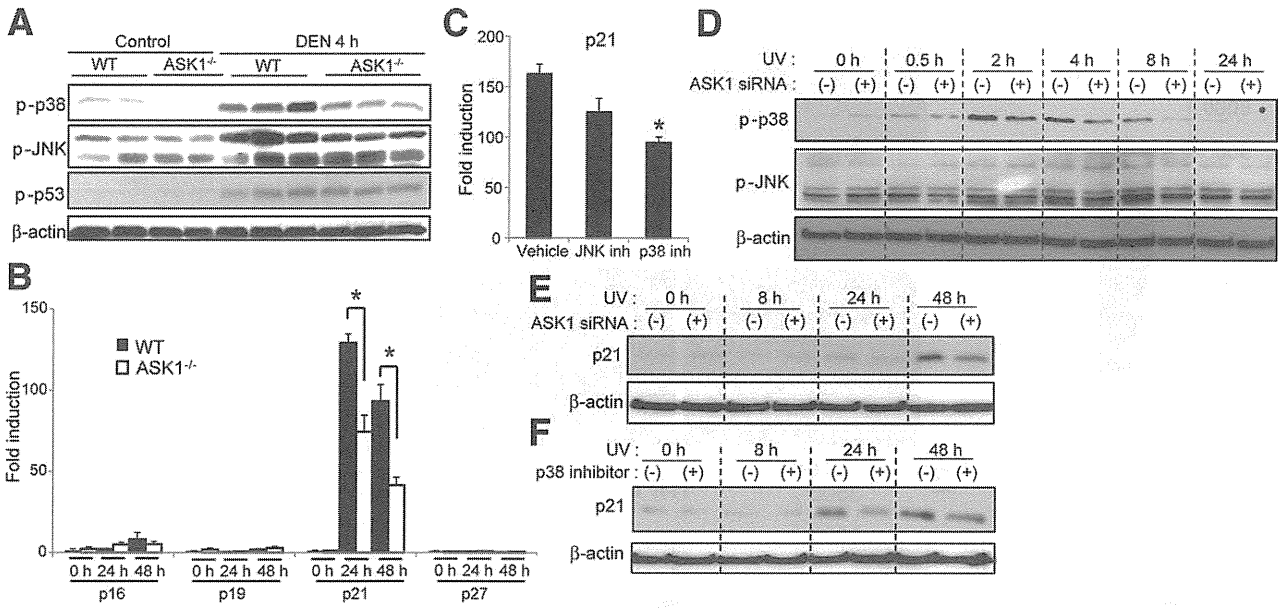

Fig. 8. Involvement of the ASK1-p38 pathway in DNA damage-induced p21 up-regulation. (A) Western blot analysis of phosphorylation of p38, JNK, and p53 in WT and ASK1$^{-/-}$ mouse livers obtained 4 hours after DEN administration (100 mg/kg). (B) mRNA levels of p16, p19, p21, and p27 were determined by real-time PCR in DEN-administered WT and ASK1$^{-/-}$ mouse livers. Data are expressed as means ± SEM (n = 4 per group). *$P < 0.05$ compared with WT mice. (C) Effect of JNK and p38 inhibitors on induction of p21 mRNA at 48 hours after DEN administration in WT mouse liver. Data are expressed as means ± SEM (n = 4 per group). *$P < 0.05$, compared with vehicle-treated mice. (D-F) The role of the ASK1-p38 pathway in p21 induction after DNA damage was analyzed by UVB irradiation (300 J/m^2 of 302-nm light) of an immortalized human normal hepatocyte line. (D) Western blot analysis of UV-induced phosphorylation of p38 and JNK in a human normal hepatocyte line after transfection with ASK1 or control siRNA. (E) Western blot analysis of the effect of ASK1 knockdown on p21 induction after UV irradiation. (F) Western blot analysis of the effect of a p38 inhibitor on p21 induction after UV irradiation. The human normal hepatocyte line was treated for 1 hour with the p38 inhibitor SB203580 (10 μM) or vehicle before UV irradiation.

p21 up-regulation. However, in addition to DNA damage, there are many other kinds of stimuli in the liver after DEN administration *in vivo*: inflammatory responses, liver regeneration signals, and toxic metabolites of DEN. Thus, we assessed the role of the ASK1-p38 pathway in p21 induction after DNA damage using UVB irradiation, which is a well-known direct DNA damage-inducer. UVB irradiation to the immortalized human normal hepatocyte line induced strong phosphorylation of p38 and very weak phosphorylation of JNK, and ASK1 silencing attenuated UVB-induced p38 phosphorylation, especially in the late phase (Fig. 8D, Supporting Fig. 5). Furthermore, UVB-induced p21 up-regulation was attenuated by ASK1 silencing and p38 inhibition (Fig. 8E F). These results suggest that ASK1 is involved in DNA damage-induced p21 up-regulation through p38 activation, and an impaired DNA damage response may be one reason for increased hepatocarcinogenesis in ASK1$^{-/-}$ mice.

Discussion

Dysregulation of the balance between cell proliferation and apoptosis plays a critical role in hepatocarcinogenesis.[31] Our results suggest that ASK1 plays only a minor role in cancer cell proliferation and a major role in death receptor-mediated apoptosis in the liver through the JNK pathway. Loss of ASK1 appears to cause an imbalance that accelerates chemical hepatocarcinogenesis in ASK1$^{-/-}$ mice. Furthermore, ASK1 is involved in the DNA damage response, through the p38 pathway. This study provides new insight into the regulation of stress-activated MAPK signaling in hepatocarcinogenesis.

JNK (primarily JNK1) has been reported to promote DEN-induced hepatocarcinogenesis by promoting cancer cell proliferation and neovascularization.[3,5] Although JNK activation was attenuated in ASK1$^{-/-}$ mice, the phenotype of ASK1$^{-/-}$ mice and JNK1$^{-/-}$ mice was opposite in hepatocarcinogenesis.[3,5] We suggest that the reasons may be as follows: (1) Although we observed attenuation of JNK activation in ASK1$^{-/-}$ HCC tissues, ASK1 appears to play only a minor role in HCC cell proliferation (Fig. 2). Additionally, vessel

density and VEGF expression in ASK1$^{-/-}$ HCC tissues were unaffected (Supporting Fig. 6A,B). Thus, the tumor-enhancing function of JNK1 seems to be preserved in ASK1$^{-/-}$ mice. (2) JNK has also been reported to act as a tumor suppressor by inducing cancer cell apoptosis.[32] JNK1 and JNK2 isoforms have distinct or redundant roles in some situations, including apoptosis induction. JNK2, but not JNK1, has been reported to play a major role in TNF-α-mediated hepatocyte apoptosis *in vivo*.[33] In our experiments using a Jo2-induced hepatitis model, the lack of neither JNK1 nor JNK2 resulted in a significant reduction in the ALT elevation or BimEL phosphorylation, unlike ASK1$^{-/-}$ mice or a pan-JNK inhibitor (Supporting Fig. 7A,B). These results suggest that the role of JNK1 and JNK2 in death receptor-mediated hepatocyte apoptosis may be redundant. Furthermore, a recent report demonstrated that JNK1 and JNK2 deficiency in hepatocytes increased DEN-induced HCC.[34] Thus, JNK1 and JNK2 have a wide range and redundant or distinct functions, and upstream molecules, such as MAP3Ks, must regulate the complex functions of JNK. We consider that ASK1 plays major roles in tumor-suppressing part of JNK in hepatocarcinogenesis. However, knockdown of ASK1 in HCC cell lines slightly decreased cell proliferation. This finding suggests that ASK1 may weakly promote the proliferation of some HCC cells, which could explain why the WT and ASK1$^{-/-}$ mice did not exhibit significant differences in tumor size.

On the other hand, mice with liver-specific p38 deficiency exhibit increased HCC development similar to ASK1$^{-/-}$ mice.[4,6] The accelerated hepatocarcinogenesis in p38-deficient mice is reportedly attributable to compensatory JNK activation and cancer cell proliferation. Although p38 activation was attenuated in ASK1$^{-/-}$ mice, JNK activation was also attenuated, unlike the liver-specific p38-deficient mice. Thus, the mechanisms of accelerated hepatocarcinogenesis in ASK1$^{-/-}$ mice and liver-specific p38-deficient mice appear to differ. p38 has also been reported to play an important role in DNA damage responses, such as cellular senescence, by inducing cyclin-dependent kinase inhibitors.[30] In this study, we showed that ASK1 is involved in DNA damage-induced p21 up-regulation through p38 activation. Furthermore, the ASK1-p38 pathway has been reported to have an inhibitory effect on malignant transformation of fibroblasts by triggering apoptosis in response to oncogene-induced reactive oxygen species (ROS).[35] Thus, the ASK1-p38 pathway may play a key role in the inhibition of tumor initiation in hepatocarcinogenesis.

Defective death-receptor signaling is considered a cause of tumor immune escape, so understanding its apoptotic mechanism is very important not only from the point of view of carcinogenesis, but also for cancer therapeutics.[21] Several *in vitro* studies have demonstrated that ASK1 is implicated in the TNF-α- and Fas-mediated apoptotic pathways,[11,36] but the *in vivo* role of ASK1 has not been determined. Our current findings provide the first evidence that ASK1 plays an important role in TNF-α- and Fas-mediated hepatocyte apoptosis *in vivo* and suggest that the JNK-Bim-mediated mitochondrial apoptotic pathway is an important downstream target of ASK1. JNK-mediated Bim phosphorylation triggers the proapoptotic activity of Bim by causing its release from sequestration to the microtubular dynein motor complex.[25] Bim initiates the mitochondrial apoptotic pathway by activating Bax and Bak directly and indirectly blocking prosurvival Bcl-2 family members.[37] Recent reports have shown that Bim plays an important role in Fas- and TNF-α-induced hepatocyte apoptosis.[19,20] Mitochondria are considered an important downstream target of ASK1 in apoptosis because overexpression of the active form of ASK1 in cell lines induces apoptosis through cytochrome *c* release from mitochondria and activation of caspase-9 and -3.[38] In our study, ASK1 was found to be involved in Fas-induced hepatocyte apoptosis but not in thymocyte apoptosis, suggesting that ASK1 is required for mitochondria-dependent apoptosis. Thus, we believe that the ASK1–JNK–Bim–mitochondrial pathway plays an important role in death receptor-mediated hepatocyte apoptosis. The observed attenuation of Bim phosphorylation and caspase-3 activation in ASK1$^{-/-}$ HCC tissues is consistent with the inhibition of death receptor-induced apoptosis.

Recently, death-receptor signaling, such as Fas signaling, has been reported to play a role in not only cancer cell apoptosis, but also cancer cell proliferation.[26] Our finding that Jo2-induced acceleration of hepatocyte proliferation after partial hepatectomy was comparable between WT and ASK1$^{-/-}$ mice suggests that ASK1 does not play a major role in Fas-mediated cell proliferation. Furthermore, the finding that WT and ASK1$^{-/-}$ HCCs exhibited no significant differences in cancer cell proliferation rates *in vivo* also supports this. Thus, ASK1 seemed to regulate the apoptotic, but not proliferative, function of JNK in Fas signaling, and ASK1$^{-/-}$ hepatocytes might alter death-receptor signaling to favor survival by escaping apoptosis. However, this is a relatively new concept, so

further study is needed to clarify the role of ASK1 in death receptor-mediated cancer cell proliferation.

In conclusion, ASK1 controls the tumor-suppressing function of stress-activated MAPK signaling, and thus acts as a tumor suppressor in hepatocarcinogenesis.

References

1. El-Serag HB, Rudolph KL. Hepatocellular carcinoma: epidemiology and molecular carcinogenesis. Gastroenterology 2007;132:2557-2676.
2. Maeda S. NF-kappaB, JNK, and TLR signaling pathways in hepatocarcinogenesis. Gastroenterol Res Pract 2010;2010:367694.
3. Sakurai T, Maeda S, Chang L, Karin M. Loss of hepatic NF-kappa B activity enhances chemical hepatocarcinogenesis through sustained c-Jun N-terminal kinase 1 activation. Proc Natl Acad Sci U S A 2006; 103:10544-10551.
4. Hui L, Bakiri L, Mairhorfer A, Schweifer N, Haslinger C, Kenner L, et al. p38alpha suppresses normal and cancer cell proliferation by antagonizing the JNK-c-Jun pathway. Nat Genet 2007;39:741-749.
5. Hui L, Zatloukal K, Scheuch H, Stepniak E, Wagner EF. Proliferation of human HCC cells and chemically induced mouse liver cancers requires JNK1-dependent p21 downregulation. J Clin Invest 2008;118: 3943-3953.
6. Sakurai T, He G, Matsuzawa A, Yu GY, Maeda S, Hardiman G, et al. Hepatocyte necrosis induced by oxidative stress and IL-1 alpha release mediate carcinogen-induced compensatory proliferation and liver tumorigenesis. Cancer Cell 2008;14:156-165.
7. Wagner EF, Nebreda AR. Signal integration by JNK and p38 MAPK pathways in cancer development. Nat Rev Cancer 2009;9:537-549.
8. She QB, Chen N, Bode AM, Flavell RA, Dong Z. Deficiency of c-Jun-NH(2)-terminal kinase-1 in mice enhances skin tumor development by 12-O-tetradecanoylphorbol-13-acetate. Cancer Res 2002;62:1343-1348.
9. Shibata W, Maeda S, Hikiba Y, Yanai A, Sakamoto K, Nakagawa H, et al. c-Jun NH2-terminal kinase 1 is a critical regulator for the development of gastric cancer in mice. Cancer Res 2008;68:5031-5039.
10. Takeda K, Noguchi T, Naguro I, Ichijo H. Apoptosis signal-regulating kinase 1 in stress and immune response. Annu Rev Pharmacol Toxicol 2008;48:199-225.
11. Ichijo H, Nishida E, Irie K, ten Dijke P, Saitoh M, Moriguchi T, et al. Induction of apoptosis by ASK1, a mammalian MAPKKK that activates SAPK/JNK and p38 signaling pathways. Science 1997;275:90-94.
12. Nakagawa H, Maeda S, Hikiba Y, Ohmae T, Shibata W, Yanai A, et al. Deletion of apoptosis signal-regulating kinase 1 attenuates acetaminophen-induced liver injury by inhibiting c-Jun N-terminal kinase activation. Gastroenterology 2008;135:1311-1321.
13. Iriyama T, Takeda K, Nakamura H, Morimoto Y, Kuroiwa T, Mizukami J, et al. ASK1 and ASK2 differentially regulate the counteracting roles of apoptosis and inflammation in tumorigenesis. EMBO J 2009; 28:843-853.
14. Hayakawa Y, Hirata Y, Nakagawa H, Sakamoto K, Hikiba Y, Otsuka M, et al. Apoptosis signal-regulating kinase 1 regulates colitis and colitis-associated tumorigenesis by the innate immune responses. Gastroenterology 2010;138:1055-1067.
15. Tobiume K, Matsuzawa A, Takahashi T, Nishitoh H, Morita K, Takeda K, et al. ASK1 is required for sustained activations of JNK/p38 MAP kinases and apoptosis. EMBO Rep 2001;2:222-228.
16. Tobiume K, Saitoh M, Ichijo H. Activation of apoptosis signal-regulating kinase 1 by the stress-induced activating phosphorylation of preformed oligomer. J Cell Physiol 2002;191:95-104.
17. Nagai H, Noguchi T, Homma K, Katagiri K, Takeda K, Matsuzawa A, et al. Ubiquitin-like sequence in ASK1 plays critical roles in the recognition and stabilization by USP9X and oxidative stress-induced cell death. Mol Cell 2009;36:805-818.
18. Saitoh M, Nishitoh H, Fujii M, Takeda K, Tobiume K, Sawada Y, et al. Mammalian thioredoxin is a direct inhibitor of apoptosis signal-regulating kinase (ASK) 1. EMBO J 1998;17:2596-2606.
19. Corazza N, Jakob S, Schaer C, Frese S, Keogh A, Stroka D, et al. TRAIL receptor-mediated JNK activation and Bim phosphorylation critically regulate Fas-mediated liver damage and lethality. J Clin Invest 2006;116:2493-2499.
20. Kaufmann T, Jost PJ, Pellegrini M, Puthalakath H, Gugasyan R, Gerondakis S, et al. Fatal hepatitis mediated by tumor necrosis factor TNF-alpha requires caspase-8 and involves the BH3-only proteins Bid and Bim. Immunity 2009;30:56-66.
21. French LE, Tschopp J. Defective death receptor signaling as a cause of tumor immune escape. Semin Cancer Biol 2002;12:51-55.
22. Walter D, Schmich K, Vogel S, Pick R, Kaufmann T, Hochmuth FC, et al. Switch from type II to I Fas/CD95 death signaling on in vitro culturing of primary hepatocytes. HEPATOLOGY 2008;48:1942-1953.
23. Faouzi S, Burckhardt BE, Hanson JC, Campe CB, Schrum LW, Rippe RA, et al. Anti-Fas induces hepatic chemokines and promotes inflammation by an NF-kappa B-independent, caspase-3-dependent pathway. J Biol Chem 2001;276:49077-49082.
24. Chen D, Zhou Q. Caspase cleavage of BimEL triggers a positive feedback amplification of apoptotic signaling. Proc Natl Acad Sci U S A 2004;101:1235-1240.
25. Lei K, Davis RJ. JNK phosphorylation of Bim-related members of the Bcl2 family induces Bax-dependent apoptosis. Proc Natl Acad Sci U S A 2003;100:2432-2437.
26. Chen L, Park SM, Tumanov AV, Hau A, Sawada K, Feig C, et al. CD95 promotes tumour growth. Nature 2010;465:492-496.
27. Desbarats J, Newell MK. Fas engagement accelerates liver regeneration after partial hepatectomy. Nat Med 2000;6:920-923.
28. Maeda S, Chang L, Li ZW, Luo JL, Leffert H, Karin M. IKKbeta is required for prevention of apoptosis mediated by cell-bound but not by circulating TNF-alpha. Immunity 2003;19:725-737.
29. Maeda S, Kamata H, Luo JL, Leffert H, Karin M. IKKbeta couples hepatocyte death to cytokine-driven compensatory proliferation that promotes chemical hepatocarcinogenesis. Cell 2005;121:977-990.
30. Thornton TM, Rincon M. Non-classical p38 map kinase functions: cell cycle checkpoints and survival. Int J Biol Sci 2009;5:44-51.
31. Fabregat I, Roncero C, Fernandez M. Survival and apoptosis: a dysregulated balance in liver cancer. Liver Int 2007;27:155-162.
32. Saxena NK, Fu PP, Nagalingam A, Wang J, Handy J, Cohen C, et al. Adiponectin modulates C-jun N-terminal kinase and mammalian target of rapamycin and inhibits hepatocellular carcinoma. Gastroenterology 2010;139:1762-1773, 1773 e1-5.
33. Wang Y, Singh R, Lefkowitch JH, Rigoli RM, Czaja MJ. Tumor necrosis factor-induced toxic liver injury results from JNK2-dependent activation of caspase-8 and the mitochondrial death pathway. J Biol Chem 2006;281:15258-15267.
34. Das M, Garlick DS, Greiner DL, Davis RJ. The role of JNK in the development of hepatocellular carcinoma. Genes Dev 2011;25:634-645.
35. Dolado I, Swat A, Ajenjo N, De Vita G, Cuadrado A, Nebreda AR. p38alpha MAP kinase as a sensor of reactive oxygen species in tumorigenesis. Cancer Cell 2007;11:191-205.
36. Chang HY, Nishitoh H, Yang X, Ichijo H, Baltimore D. Activation of apoptosis signal-regulating kinase 1 (ASK1) by the adapter protein Daxx. Science 1998;281:1860-1863.
37. Youle RJ, Strasser A. The BCL-2 protein family: opposing activities that mediate cell death. Nat Rev Mol Cell Biol 2008;9:47-59.
38. Hatai T, Matsuzawa A, Inoshita S, Mochida Y, Kuroda T, Sakamaki K, et al. Execution of apoptosis signal-regulating kinase 1 (ASK1)-induced apoptosis by the mitochondria-dependent caspase activation. J Biol Chem 2000;275:26576-26581.

nature COMMUNICATIONS

ARTICLE

Received 30 Mar 2011 | Accepted 11 May 2011 | Published 7 Jun 2011

DOI:10.1038/ncomms1345

MicroRNA122 is a key regulator of α-fetoprotein expression and influences the aggressiveness of hepatocellular carcinoma

Kentaro Kojima[1,*], Akemi Takata[1,*], Charles Vadnais[2,*], Motoyuki Otsuka[1], Takeshi Yoshikawa[1], Masao Akanuma[3], Yuji Kondo[1], Young Jun Kang[4], Takahiro Kishikawa[1], Naoya Kato[5], Zhifang Xie[6], Weiping J. Zhang[6], Haruhiko Yoshida[1], Masao Omata[1], Alain Nepveu[2] & Kazuhiko Koike[1]

α-fetoprotein (AFP) is not only a widely used biomarker in hepatocellular carcinoma (HCC) surveillance, but is also clinically recognized as linked with aggressive tumour behaviour. Here we show that deregulation of microRNA122, a liver-specific microRNA, is a cause of both AFP elevation and a more biologically aggressive phenotype in HCC. We identify CUX1, a direct target of microRNA122, as a common central mediator of these two effects. Using liver tissues from transgenic mice in which microRNA122 is functionally silenced, an orthotopic xenograft tumour model, and human clinical samples, we further demonstrate that a microRNA122/CUX1/microRNA214/ZBTB20 pathway regulates AFP expression. We also show that the microRNA122/CUX1/RhoA pathway regulates the aggressive characteristics of tumours. We conclude that microRNA122 and associated signalling proteins may represent viable therapeutic targets, and that serum AFP levels in HCC patients may be a surrogate marker for deregulated intracellular microRNA122 signalling pathways in HCC tissues.

[1] Department of Gastroenterology, Graduate School of Medicine, The University of Tokyo, Tokyo 113-8655, Japan. [2] Goodman Cancer Center and Departments of Oncology, Biochemistry and Medicine, McGill University, Montreal, Quebec H3A 1A3, Canada. [3] Division of Gastroenterology, The Institute for Adult Diseases, Asahi Life Foundation, Tokyo 100-0005, Japan. [4] Department of Immunology and Microbial Science, The Scripps Research Institute, La Jolla, California 92037, USA. [5] Unit of Disease Control Genome Medicine, The Institute of Medical Science, The University of Tokyo, Tokyo 108-8639, Japan. [6] Department of Pathophysiology, Second Military Medical University, Shanghai 200433, China. *These authors contributed equally to this work. Correspondence and requests for materials should be addressed to M. Otsuka (email: otsukamo-tky@umin.ac.jp).

The incidence of hepatocellular carcinoma (HCC), the third most common cause of cancer-related mortality worldwide[1], is currently increasing[2]. The recent discovery of the efficacy of sorafenib, a multikinase inhibitor, as a treatment for patients with advanced HCC, has represented a major breakthrough in the clinical management, although the survival benefit has been shown to be less than 3 months[3]. No other effective therapy is currently available for patients with advanced disease[4]. As such, there is a continuing need to develop novel therapeutics and approaches for treatment of advanced HCC[5].

To develop targeted cancer therapies, we must first identify aberrantly regulated molecular pathways specific to this cancer. Clinically, it is also important to discover useful and convenient surrogate serum biomarkers that reflect aberrations in molecular pathways due to the molecular mechanisms of their expression, to identify the deregulated intracellular signalling pathways and to spare the patients from invasive clinical tests.

Currently, α-fetoprotein (AFP) is the most widely used serum biomarker for HCC surveillance[6]. Although the regulation of AFP gene expression is not fully understood, p53 (ref. 7), β-catenin[8] and the recently identified zinc-finger protein, ZBTB20 (ref. 9), have been reported to be involved. Furthermore, whereas mounting clinical evidence indicates that AFP elevation is linked to a more aggressive tumour phenotype characterized by vascular invasion, metastasis and poor differentiation[10,11], it remains to be determined whether the two phenotypes represent anything more than coincidental epiphenomena[12].

MicroRNAs (miRNAs) are short, single-stranded, non-coding RNAs. Although first identified in *Caenorhabditis elegans*[13], miRNAs are now known to be expressed in most organisms, from plants to vertebrates[14]. Primary miRNAs, which possess stem-loop structures, are processed into mature miRNAs by Drosha and Dicer RNA polymerase III. These mature miRNAs then associate with the RNA-induced silencing complex, and the resulting complex directly binds to the 3′-untranslated regions of target messenger RNAs to act as suppressors of translation and gene expression. Thus, depending on the target mRNAs, miRNAs are responsible for the control of various biological functions including cell proliferation, apoptosis, differentiation, metabolism, oncogenesis and oncogenic suppression[15–17].

MiRNA122 (miR122) is a tissue-specific miRNA that is most abundant in the liver[18], wherein it is responsible for the maintenance of fatty acid metabolism[19,20] and circadian rhythms[21]. As shown for other tissue-specific miRNAs[22], expression of miR122 has been reported to be downregulated in carcinomas, particularly in more malignant tumours, although these results remain controversial because of conflicting reports[23–26]. The biological significance of the downregulation of miR122 expression in HCC at the molecular level has not yet been fully elucidated.

In the present study, we explored the role of microR122 in HCC by silencing it both in human HCC cells and in a transgenic mouse model. Our molecular analysis enabled us to define the complex regulatory cascades underlying the clinically recognized link between raised AFP levels and a more aggressive phenotype in HCC.

Results

Establishment of miR122-silenced HCC cell lines. To characterize the functional consequences of miR122 downregulation in HCC cells, Huh7 and PLC/PRF/5 cells were stably transduced with a lentivirus that expresses RNA hairpins that produce mature antisense RNA designed to silence miR122 function. These cells were selected on the basis of their relatively high levels of miR122 expression[24,27]. Several mismatches were intentionally inserted into the RNA hairpin sequences to produce more stable templates for miR122 binding and sequestration and to perturb the participation of miR122 in RNA-induced silencing complex-associated inhibition of translation (Fig. 1a).

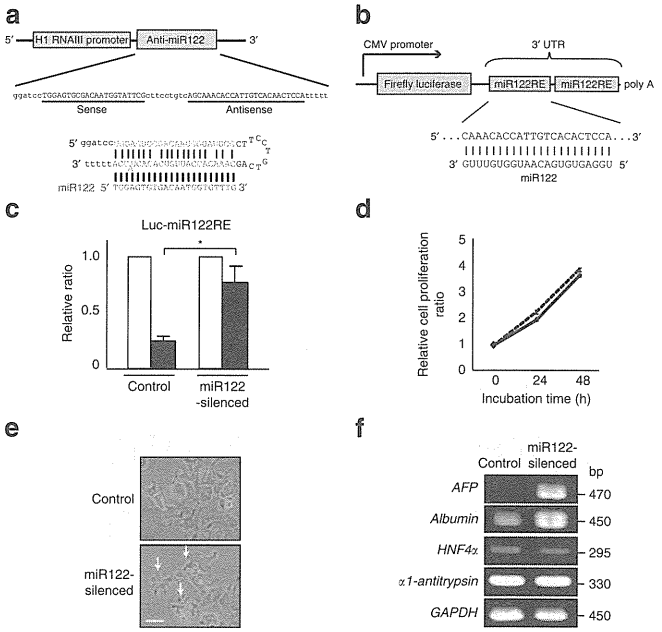

Figure 1 | Establishment of miR122-silenced HCC cell lines. (**a**), The miRZip122 construct, which yields a functional single-stranded full-length antisense miRNA complementary o miR122, processed from a stem-loop-stem molecule and transcribed from the constitutively active H1 RNA III promoter. Several mismatched nucleotides were included to efficiently produce a single-stranded antisense miR122 molecule. (**b**) Schematic representation of the luciferase reporter used to examine miR122 activity. The firefly luciferase gene, driven by a cytomegalovirus (CMV) promoter, contains two tandem miR122-binding sites (miR122-responsive elements; miR122-RE) in its 3′-UTR. (**c**) The suppressive effects of miR122 precursor expression (black bar) on luciferase activity in control and miR122-silenced cells. Test values were normalized to those obtained from the cells transfected with a miRNA precursor-non-expressing empty vector (white bar), which were set to 1. Data represent the mean±s.d. of three independent experiments using Huh7 cells. $*P<0.05$ (*t*-test). Similar results were obtained using PLC/PRF/5 cells. (**d**) Control (solid line) and miR122-silenced cells (dashed line) were plated at a density of 2×10^4 cells per well. After incubation for 24 and 48 h, numbers of cells were calculated as described in the Methods. Data represent the mean±s.d. of three independent experiments using Huh7 cells. Similar results were obtained using PLC/PRF/5 cells. (**e**) Changes in cellular morphology of Huh7 miR122-silenced cells are shown. Arrows indicate pseudopodia. Scale bar, 50 μm. Similar phenotypes were observed using PLC/PRF/5 cells. (**f**) The expression of several hepatocyte markers in control and Huh7 miR122-silenced cells was evaluated by semi-quantitative RT-PCR. Representative results from three independent experiments using Huh7 cells are shown. Similar results were obtained using PLC/PRF/5 cells.

To confirm effective miR122 silencing in transduced cells, we analysed the luciferase activity of reporters containing miR122-binding sites (the function of which is suppressed by miR122 overexpression) (Fig. 1b) in miR122-silenced and control cells. As expected, overexpression of the miR122 precursor greatly suppressed luciferase activity in control cells (Fig. 1c). In contrast, this suppressive effect was significantly reduced in miR122-silenced cells (Fig. 1c), indicating that miR122 was indeed functionally silenced.

To characterize the biological changes that result from the loss of miR122 function, we next analysed cell proliferation, morphology and differentiation in miR122-silenced cells. The rates of cell

proliferation were comparable between control and silenced cells (Fig. 1d); however, miR122-silenced cells exhibited a larger number of distinct pseudopodia (Fig. 1e). Next, as miR122 is specifically expressed in the liver, we hypothesized that it may have a role in hepatocyte differentiation and, therefore, we investigated the expression of several hepatocyte markers by semi-quantitative RT–PCR. We observed an increase in AFP expression and a slight elevation of albumin expression in miR122-silenced cells, but the expression levels of other hepatocyte markers, such as hepatocyte nuclear factor 4α (HNF4α) and α_1-antitrypsin, did not change (Fig. 1f).

MiR122-silenced HCC cells exhibit a more invasive phenotype. Because miR122-silenced cells exhibited an increased number of pseudopodia, we next characterized phenotypes associated with more biologically aggressive cell characteristics. We found that actin polymerization and pseudopod formation were significantly increased in miR122-silenced cells (Fig. 2a). The increase in the number of pseudopodia was confirmed by a quantitative pseudopodia assay (Supplementary Fig. S1). Although the expression levels of the mesenchymal marker α-smooth muscle actin were only slightly increased, we observed a significant decrease in the expression of the epithelial marker E-cadherin in miR122-silenced cells (Fig. 2b). Furthermore, the expression of other epithelial-to-mesenchymal transition markers such as fibronectin, N-cadherin, snail and Zeb1 was altered in miR122-silenced cells (Supplementary Fig. S1). These findings are consistent with the notion that loss of miR122 function leads to a more malignant phenotype.

We next performed scratch and invasion assays to characterize the invasive phenotype of miR122-silenced cells. Rates of cell migration and of cell invasion were significantly increased in miR122-silenced cells (Fig. 2c,d). As the proliferation rates of control and miR122-silenced cells were similar (Fig. 1d), altogether these results suggest that inhibition of miR122 function in HCC cells may lead to increases in malignancy-related cellular properties.

To investigate the molecular mechanisms underlying these cellular phenotypes, we assessed the activity of RhoA and Rac1, which are small GTPases that are closely associated with cell migration and invasion[28]. Although Rac1 activity did not significantly change, RhoA activity significantly increased in miR122-silenced cells (Fig. 2e), suggesting that the increase in cell migration and invasion in miR122-silenced cells may result from increased RhoA activity.

AFP expression is increased in miR122-silenced HCC cells. As we observed an increase in AFP expression in miR122-silenced cells (Fig. 1f), we next sought to quantify AFP concentrations in culture supernatants using an enzyme-linked immunosorbent assay (ELISA). AFP levels were approximately three times higher in the supernatant of miR122-silenced cells as compared with control cells (Fig. 3a). Consistent with this observation, immunofluorescence staining for AFP produced a stronger cytoplasmic signal and quantitative RT–PCR revealed a tenfold increase in AFP mRNA levels in miR122-silenced cells (Fig. 3b,c).

The 3′-UTR of the AFP mRNA did not contain predicted miR122 target sequences, based on sequence analyses performed using miRNA target search engines such as TargetScan (http://www.targetscan.org), suggesting that it is unlikely that miR122 directly regulates AFP expression. Therefore, to characterize the mechanisms underlying increased AFP expression in miR122-silenced cells, we first assessed the stability of the AFP mRNA in miR122-silenced cells. As expected, AFP mRNA stability was unaffected by silencing of miR122, as the amount of mRNA was comparable between control and miR122-silenced cells at 6, 12 and 24 h after inhibition of new transcription by treatment with actinomycin D (Fig. 3d). The increase in AFP mRNA levels in the absence of changes in mRNA stability suggested that transcription of AFP was increased

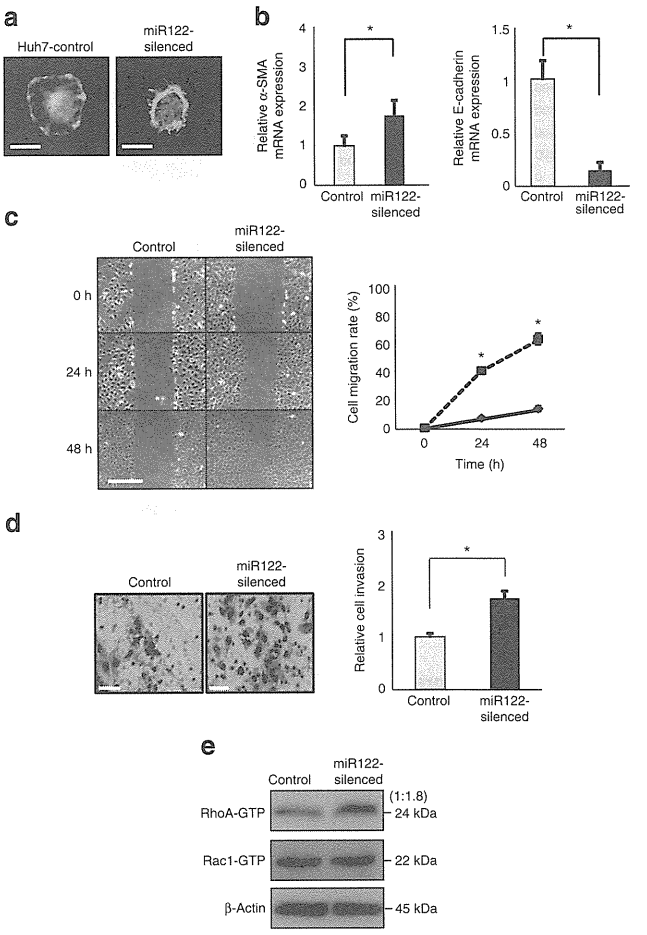

Figure 2 | HCC cells silenced for miR122 function exhibit a more invasive phenotype. (**a**) Cells were treated with 2 ng ml^{-1} TGF-β for 12 h, and actin filaments were stained with Alexa Fluor 488-conjugated phalloidin. Representative results from two independent experiments using Huh7 cells are shown. Similar results were obtained using PLC/PRF/5 cells. Scale bar, 50 μm. (**b**) Expression levels of α – smooth muscle actin and E-cadherin mRNAs were assessed by quantitative RT–PCR. Values shown represent mRNA expression levels in experimental cells relative to control cells. Data represent the mean ± s.d. of three independent experiments using Huh7 cells. *P < 0.05 (t-test). Similar results were obtained for PLC/PRF/5 cells. (**c**) The degree of cell migration was characterized using a scratch assay. The ratio of migrating cells was significantly increased in miR122-silenced cells at 24 and 48 h after scratching. Left panels show representative images. Right panel shows the results from cell counts for four randomly chosen fields per experiment. Data are represented as the mean ± s.d. of three experiments using Huh7 control (solid line) and miR122-silenced cells (dashed line). *P < 0.001 (t-test). Similar results were obtained for PLC/PRF/5 cells. (**d**) The degree of cell invasion was examined using cell invasion chambers. Representative images of stained invaded cells (left). The relative cell invasion ratio after normalization to control cell invasion levels (right). Data represent the mean ± s.d. of three independent experiments using Huh7 cells. Scale bar, 100 μm. *P < 0.01 (t-test). Similar results were obtained for PLC/PRF/5 cells. (**e**) Rho and Rac1 activity was determined by comparing the amounts of active GTP-bound RhoA (RhoA-GTP) and Rac1 (Rac1-GTP) between control and miR122-silenced cells. The indicated numbers represent the relative expression levels. Equal loading in pull-down assays was confirmed by analysis of β-actin levels in the cell lysates. Representative results of five independent experiments using Huh7 cells are shown. Similar results were obtained using PLC/PRF/5 cells.

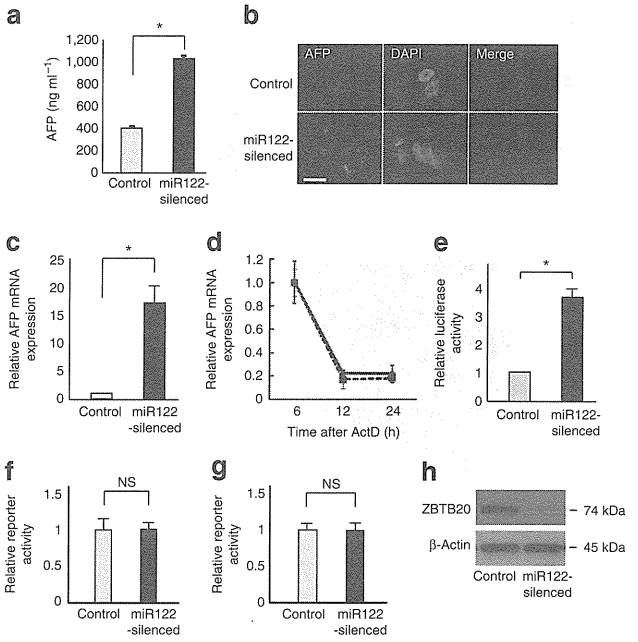

Figure 3 | Increased expression of AFP in HCC cells silenced for miR122 function. (**a**) The AFP concentration in the culture medium was determined by ELISA. Data represent the mean±s.d. of three independent experiments using Huh7 cells. *$P<0.01$ (*t*-test). Similar results were obtained for PLC/PRF/5 cells. (**b**) Immunofluorescent staining for AFP in the cytoplasm of control and miR122-silenced Huh7cells. Representative images of stained cells from three independent experiments are shown. Scale bar, 50 μm. (**c**) Amounts of AFP mRNA in Huh7 control and miR122-silenced cells were determined by quantitative RT-PCR. Data represent the mean±s.d. of three independent experiments. *$P<0.05$ (*t*-test). Similar results were obtained using PLC/PRF/5 cells. (**d**) AFP mRNA stability in Huh7 control (solid line) and miR122-silenced (dashed line) cells was determined by quantitative RT-PCR at 6, 12, and 24 h after treating cells with 10 μl ml^{-1} actinomycin D. Data represent the mean±s.d. of three independent experiments. Similar results were observed using PLC/PRF/5 cells. (**e**) AFP promoter activity was measured in reporter assays using Huh7 cells and AFP promoter-luciferase construct. Data represent the mean±s.d. of three independent experiments. *$P<0.05$ (*t*-test). Similar results were obtained using PLC/PRF/5 cells. (**f**, **g**) Luciferase assays were performed using reporter plasmids to measure p53 (**f**) and β-catenin (**g**) activities. Data represent the mean±s.d. of three independent experiments. Similar results were obtained using PLC/PRF/5 cells. (**h**) ZBTB20 protein levels in miR122-silenced cells. A representative result from three independent experiments using Huh7 cells is shown. Similar results were obtained using PLC/PRF/5 cells.

in miR122-silenced cells as a result of increased AFP promoter activity. Indeed, AFP promoter activity was almost four times higher in miR122-silenced cells than in control cells, as assessed by a reporter assay (Fig. 3e).

Because AFP promoter activity is in part regulated by p53 (ref. 7), we assessed p53 activity using reporter constructs. However, no changes in p53 activity were detected in miR122-silenced cells (Fig. 3f). As mutation of β-catenin has also been reported to be involved in upregulation of AFP expression[8], we next analysed β-catenin activity in miR122-silenced cells. Similar to p53, no change in β-catenin activity was evident in miR122-silenced cells compared with control cells (Fig. 3g).

Recently, it was reported that ZBTB20 acts as a repressor of AFP transcription[9]. This result led us to assess the expression of the ZBTB20 protein in miR122-silenced cells. Indeed, western blot analysis revealed that ZBTB20 expression was decreased in miR122-silenced cells (Fig. 3h). However, as ZBT20 lacks the presence of predicted miR122 target sequences based on computational searches of the 3′-UTR, it was also unlikely that miR122 directly regulates ZBTB20 expression. These observations suggest that other indirect mechanisms may lead to decreased ZBTB20 expression in miR122-silenced cells.

CUX1 is the regulator of phenotypes in miR122-silenced cells. To explore the mechanisms by which miR122 regulates cell motility, invasion and AFP expression, we used computational searches to identify potential miR122 target genes with known functions related to these processes. This analysis led to the identification of Cut homeobox 1 (CUX1, also known as CCAAT-displacement protein/cut homeobox, CDP/Cux/Cut) through the presence of a high probability miR122 target site located in the 3′-UTR and a perfect match in the seed sequences. CUX1 is a transcription factor that regulates multiple processes including cell cycle progression, chromosomal segregation and cell migration[29,30]. Consistent with the effects of miR122 silencing described above, CUX1 was reported to modulate cell motility and invasion through the control of RhoA activity[31–33]. We observed that whereas CUX1 mRNA levels remained unchanged (Fig. 4a), there was a significant increase in the steady-state level of the CUX1 p200 and p110 isoforms in miR122-silenced cells (Fig. 4b).

To investigate the contribution of CUX1 upregulation to the increase in AFP expression and invasive properties observed in miR122-silenced cells, we knocked down CUX1 protein expression using lentiviruses expressing CUX1 short hairpin RNAs (shRNAs) (Fig. 4c). In the resulting double-knockdown cells, AFP protein expression in cell-culture supernatant and cell invasion were both reduced to levels similar to that of the parental Huh7 cells (Fig. 4d–f).

CUX1 represses ZBTB20 expression via miR214. We next assessed whether miR122 directly targets CUX1 by constructing a luciferase reporter construct that possessed a portion of the CUX1 3′-UTR containing the putative miR122 target site (Fig. 5a). Co-transfection experiments revealed that luciferase activity was suppressed by overexpression of a miR122 precursor-expressing plasmid (Fig. 5b). This suppressive effect was prevented by introducing two point mutations into the seed sequences of the miR122 target site (Fig. 5a,b), demonstrating that miR122 directly targets these sequences.

To confirm these effects, we generated 293T cell lines that stably expressed the miR122-precursor construct by transducing cells with miR122 precursor-expressing lentiviruses tagged with green fluorescent protein (Supplementary Fig. S2a). As expected, the anti-miR122 construct did not affect control 293T cells, owing to the lack of miR122 expression. However, the anti-miR122 construct greatly enhanced luciferase activity in 293T cells stably expressing the miR122-precursor, confirming that miR122 was transduced into the 293 T cells (Supplementary Fig. S2b). Consistent with the results described above, these cells exhibited decreased expression of CUX1, particularly the p200 isoform, and also showed a modest, but reproducible, increase in ZBTB20 expression (Fig. 5c). These results suggest that miR122 directly regulates CUX1 protein expression, which in turn may regulate ZBTB20 expression.

Because CUX1 can function as a transcriptional modulator[29], we initially hypothesized that CUX1 is a direct regulator of ZBTB20 transcription. However, quantitative RT–PCR analysis revealed that levels of the ZBTB20 mRNA were unchanged in miR122-silenced cells compared with controls (Fig. 5d). To explain the discrepancy between unchanged levels of ZBTB20 mRNA and decreases in protein expression levels in miR122-silenced cells, we searched for miRNAs that could potentially target the ZBTB20 3′-UTR. Based on computational searches, miR214 and miR375 were identified as candidate ZBTB20-regulatory miRNAs. Although levels of miR375 were unchanged in miR122-silenced cells (Fig. 5e), expression of miR214 was significantly increased (Fig. 5e).

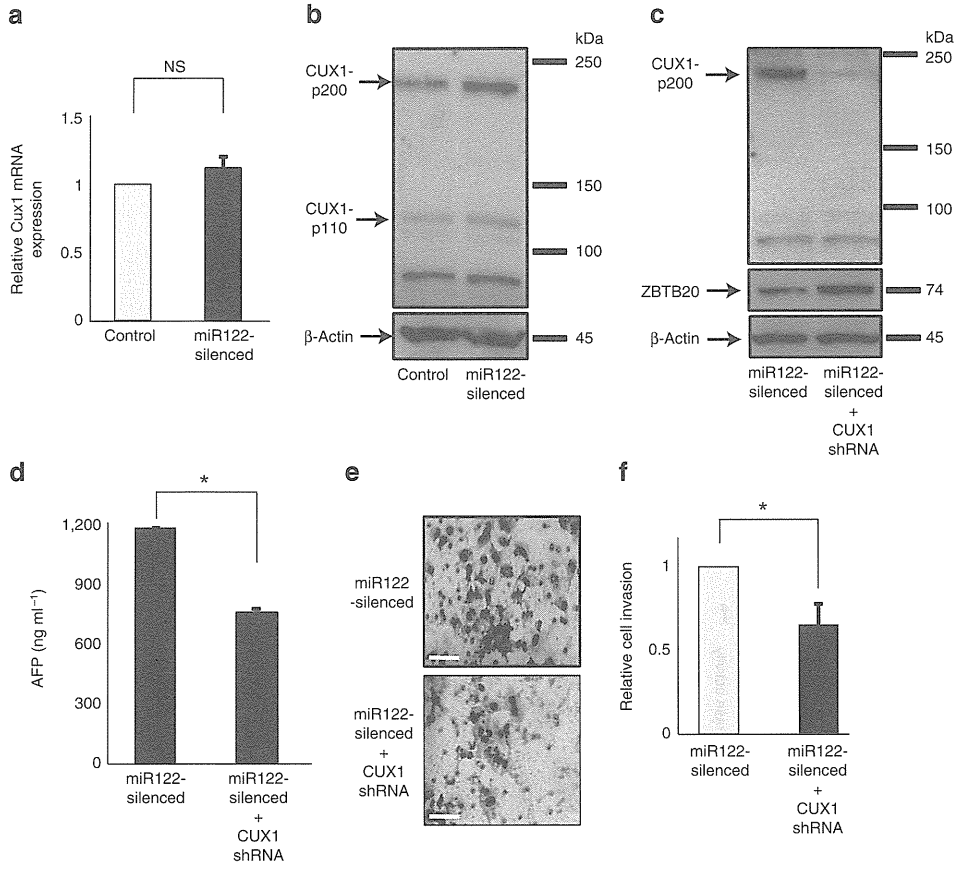

Figure 4 | CUX1-mediated regulation of AFP expression and phenotypic changes in miR122 functionally silenced cells. (**a**) CUX1 mRNA levels in control and miR122-silenced cells were analysed by quantitative RT–PCR. Data represent the mean±s.d. of three independent experiments using Huh7 cells. (**b**) p200 and p110 CUX1 protein levels were increased in miR122-silenced cells compared with control cells. A representative result from three independent experiments using Huh7 cells is shown. Similar results were obtained for PLC/PRF/5 cells. (**c**) CUX1 and ZBTB20 protein expression in double CUX1/miR122 knockdown Huh7 cells. Similar results were obtained using PLC/PRF/5 cells. (**d**) AFP concentrations in the culture medium supernatants were determined by ELISA. Data represent the mean±s.d. of three independent experiments. *$P<0.01$ (*t*-test). Similar results were observed using PLC/PRF/5 cells. (**e**, **f**) The change of cell invasion ratio by CUX1 knockdown in miR122-silenced Huh7 cells. Representative images of stained invading cells are shown (**e**). The relative cell invasion ratio after normalization to control invasion levels is shown (**f**). Data represent the mean±s.d. of three independent experiments. Scale bar, 100 μm. *$P<0.01$ (*t*-test). Similar results were obtained using PLC/PRF/5 cells.

To assess whether miR214 directly targeted the ZBTB20 3′-UTR, we constructed a luciferase reporter with the region of the ZBTB20 3′-UTR that contains the putative miR214 target site. Reporter assays revealed that luciferase activity was indeed suppressed by overexpression of the miR214 precursor, suggesting that miR214 directly targets the ZBTB20 3′-UTR and suppresses its expression (Fig. 5f). Consistent with these findings, cells that stably overexpressed the miR214 precursor exhibited decreased levels of ZBTB20 protein expression (Fig. 5g).

The putative promoter regions of miR214 contain multiple CUX1 binding sites as revealed by MATCH, a transcription factor binding site search engine (http://www.gene-regulation.com). A scanning chromatin immunoprecipitation (ChIP) experiment, followed by real-time PCR, using a series of primer pairs, confirmed that CUX1 binds to multiple genomic sites in the miR214 promoter region (Fig. 6a). We therefore hypothesized that CUX1 may regulate miR214 transcription. Consistent with this notion, we found that miR214 expression was decreased in CUX1 knockdown Huh7 cells (Fig. 6b). The role of CUX1 as an activator of miR214 transcription was further verified by knocking down or overexpressing CUX1 in another cell line. Levels of miR214 decreased following the constitutive knockdown of CUX1 with shRNA (Fig. 6c). In contrast, retroviral infection with a vector expressing p110 CUX1 led to an increase in miR214 (Fig. 6d). These findings were confirmed using doxycycline-inducible CUX1 shRNA. As previously observed for other transcriptional targets of CUX1 (refs 30,34), levels of miR214 were reduced in the presence of doxycycline, and then returned to levels higher than in untreated cells upon removal of the doxycycline inducer miR214 (Fig. 6e).

Next, to assess the contribution of miR214 to the control of ZBTB20 expression in miR122-silenced cells, we measured ZBTB20 expression after parallel silencing of miR214 in miR122-silenced cells. Although ZBTB20 protein expression was reduced by almost 50% by miR122 silencing, it was restored to >90% of control levels by miR214 silencing (Supplementary Fig. S3). Thus, CUX1-induced miR214 regulates, at least in part, ZBTB20 expression in miR122-silenced cells, leading to the upregulation of AFP expression.

Regulation of of CUX1 and AFP expression by miR122 was also confirmed in other HCC cell lines in which miR122 was overexpressed or silenced. Northern blotting showed that the expression of miR122 was relatively low in Hep3B and HepG2 cells, but was relatively high in Huh1, Huh7 and PLC/PRF/5 cells (Supplementary Fig. S4a). We therefore overexpressed the miR122 precursor in Hep3B and HepG2 cells and silenced miR122 in Huh1, Huh7 and PLC/PRF/5 cells (Supplementary Fig. S4b). CUX1 expression was respectively suppressed and enhanced by miR122 precursor overexpression and miR122 silencing (Supplementary Fig. S4c). In contrast, AFP expression was respectively enhanced and suppressed

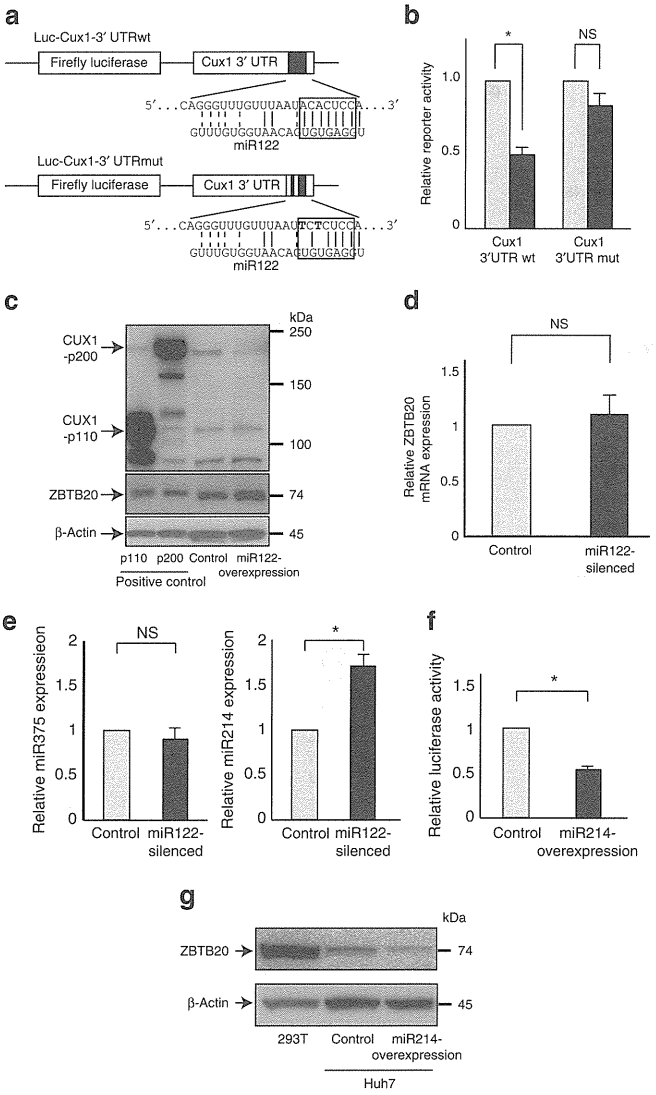

Figure 5 | MiR122 directly targets CUX1. (**a**) A luciferase reporter carrying a region of the wild type CUX1 3′UTR containing the putative miR122 target site (Luc-CUX1-3′UTRwt) was used to assess the effects of miR122 on expression of CUX1. A second luciferase reporter with two nucleotide mutations (indicated in bold) in the seed sequences (indicated by a rectangle) of the putative miR122 target sites (Luc-CUX1-3′UTRmut) was also utilized to assess specificity. (**b**) Huh7 cells were co-transfected with Luc-CUX1-3′UTRwt or Luc-CUX1-3′UTRmut and either an empty control vector (white bar) or a miR122 precursor expression plasmid (black bar). Data represent the mean±s.d. of three independent experiments. *$P<0.05$ (*t*-test). (**c**) CUX1 and ZBTB20 expression in 293 T cells-expressing the miR122 precursor. Cell lysates transiently transfected with CUX1 p200 or p110 expression plasmids were used as positive controls. Representative results from four independent experiments are shown. (**d**) ZBTB20 mRNA levels in miR122-silenced Huh7 cells were determined by quantitative RT-PCR. Data represent the mean±s.d. of three independent experiments. Similar results were obtained using PLC/PRF/5 cells. (**e**) Levels of miR375 (left) and miR214 (right) in miR122-silenced Huh7 cells were analysed by quantitative RT-PCR. Data represent the mean±s.d. of three independent experiments. *$P<0.05$ (*t*-test). (**f**) Huh7 cells were co-transfected with Luc-ZBTB20-3′UTR and either an empty control vector or an miR214 precursor expression plasmid. Data represent the mean±s.d. of three independent experiments. *$P<0.05$ (*t*-test). (**g**) ZBTB20 expression was decreased in Huh7 miR214-overexpressing cells. 293T cell lysate was used as a positive control. Representative results from four independent experiments are shown.

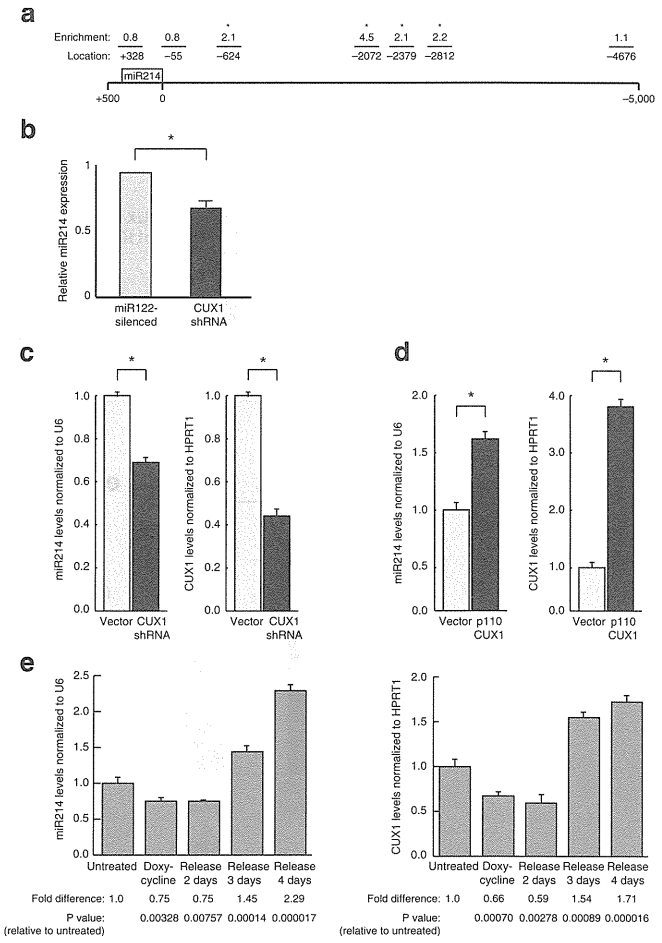

Figure 6 | CUX1 regulated miR-214 expression. (**a**), CUX1 enrichment at the miR214 locus. ChIP assays were performed using Hs578T cells. Fold enrichment and location of the center of each qPCR amplicon are shown. *$P<0.05$ (*t*-test). (**b**) MiR214 expression levels after CUX1 knockdown in miR122-silenced Huh7 cells were determined by quantitative RT-PCR. Data represent the mean±s.d. of three independent experiments. *$P<0.05$ (*t*-test). Similar results were obtained using PLC/PRF/5 cells. (**c**) Levels of miR214 and CUX1 RNA in Hs578T cells infected with an empty vector or a lentiviral vector constitutively expressing CUX1 shRNA. Data represent the mean±s.d. of three independent experiments. *$P<0.05$ (*t*-test). (**d**) Hs578T cells were infected with a retrovirus expressing p110 CUX1. Levels of miR214 and CUX1 mRNA were measured 1 day later. Data represent the mean±s.d. of three independent experiments. *$P<0.05$ (*t*-test). (**e**) Levels of miR214 and CUX1 mRNA in Hs578T cells expressing a doxycycline-inducible CUX1 shRNA. Levels are shown prior to treatment, after 5 days of doxycycline treatment, and 2, 3 and 4 days after withdrawal of doxycycline. Fold changes with the mean±s.d. of three independent experiments and *P*-values are shown (*t*-test).

(Supplementary Fig. S4d), confirming that AFP expression is regulated by an miR122-CUX1 pathway in multiple HCC cell lines.

These results indicate that functional silencing of miR122 leads to an increase in CUX1 protein expression, resulting in repression of ZBTB20 through an increase in miR214 expression. Repression of ZBTB20, in turn, leads to an increase in AFP expression. Because CUX1 is a modulator of cell motility and invasion[35–37], upregulation of this protein also enhances RhoA activity, increasing the malignant properties of cancer cells.

Expression of CUX1-related molecules in miR122-silenced mice. To explore the pathway delineated above in an *in vivo* model, we gen-

erated transgenic mice expressing antisense miR122 under the control of an H1 promoter (Fig. 7a) to inhibit the function of endogenous miR122 (ref. 38). *In situ* hybridization analysis in these mice revealed weak miR122 staining in liver tissue in comparison with control mice, likely due to binding of the anti-sense miR122 to endogenous miR122, which produces a double-stranded DNA and likely inhibits hybridization of the probe (Fig. 7b). Although structural development of the liver appeared normal based on haematoxylin and eosin staining (Supplementary Fig. S5), AFP mRNA expression (Fig. 7c) and p200 and p110 CUX1 protein expression were upregulated in the liver of anti-miR122 transgenic mice (Fig. 7d). Moreover, whereas levels of ZBTB20 mRNA were unchanged, ZBTB20 protein expression was decreased in the liver (Fig. 7d), in agreement with *in vitro* results demonstrating the regulation of ZBTB20 at the translational level (Fig. 5c,d). This was associated with a significant increase in the levels of miR214 in anti-miR122 transgenic mice (Fig. 7e). Thus, results from mouse liver tissue confirm that the miR122/CUX1/miR214/ZBTB20 regulatory pathway is also functional in an *in vivo* model.

Invasiveness of miR122-silenced cells in xenograft model. Next, we transplanted control and miR122-silenced PLC/PRF/5 cells under the liver capsule of nude mice (Fig. 7f) to determine whether miR122 silencing in HCC actually produces a more malignant phenotype *in vivo*. PLC/PRF/5 cells were chosen because of their transplantability in nude mice[39]. Neither intrahepatic metastases nor vascular invasion were detected in the livers of mice transplanted with control cells at 4 weeks post-transplantation. In contrast, vascular invasion was observed in the livers of mice transplanted with miR122-silenced HCC cells (Fig. 7g). These results suggest that miR122 silencing in HCC leads to a more aggressive phenotype.

HCC staging and the expression of miR122-related molecules. To assess the relevance of these results to human disease, we examined miR122 and AFP expression in several clinical-grade human HCC samples. We analysed miR122 expression by *in situ* hybridization (Fig. 8a) and AFP expression by immunohistochemistry (Fig. 8b). Both AFP expression and malignancy grading were inversely correlated with miR122 expression levels (Fig. 8c,d). In addition, CUX1, miR214 and ZBTB20 expression was also correlated with miR122 expression, as determined using serial sections (Supplementary Fig. S6a, b and c). These results, together with our studies in tissue culture systems and a transgenic mouse model, suggest that a reduction in the expression of miR122 increases AFP expression via a miRNA122-CUX1-miRNA214-ZBTB20 pathway and that the development of more biologically aggressive forms of HCC occurs via a miRNA122-CUX1-RhoA pathway (Supplementary Fig. S7). The miRNA-mediated mechanism described in this report may explain the clinically known link between increased AFP levels and more biologically aggressive cell characteristics in HCC.

Discussion

High AFP levels have been clinically shown to be an unfavourable prognostic factor in HCC patients[40]. In this study, we demonstrate that reduced expression of miR122 in HCC cells contributes to elevated AFP expression and, subsequently, a more aggressive phenotype. These results provide a molecular framework that explains the reported link between elevated AFP levels and a poor clinical outcome in HCC patients.

Clinically, high AFP expression is correlated with more biologically aggressive properties of HCC, as patients with high AFP levels have a significantly higher frequency of portal vein invasion and intrahepatic metastases. Additionally, these patients display significantly lower rates of recurrence-free survival and a trend towards lower overall survival[41]. In the present study, we have presented several lines of evidence indicating that decreased expression of miR122 in HCC leads to the two phenomena that

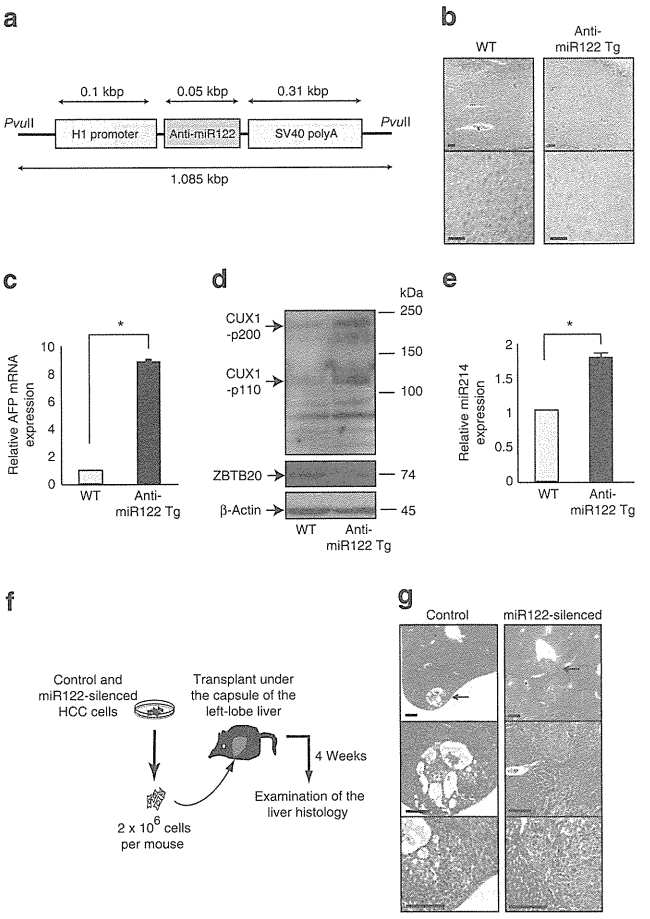

Figure 7 | AFP expression is increased in the liver of anti-miR122 transgenic mice. (**a**) DNA construct used to establishment transgenic mice in which miR122 is functionally silenced (anti-miR122 transgenic mice). This construct (like the construct used in the *in vitro* studies) generates a functional single-stranded full-length antisense miRNA complementary to miR122. (**b**) Confirmation of the expression of an antisense RNA directed against miR122 in anti-miR122 transgenic (anti-miR122 Tg) mice. Amounts of miR122 detected by *in situ* hybridization (blue/purple staining) in the liver tissues of anti-miR122 transgenic mice and WT mice. Results shown are representative of three independent experiments performed using littermates from four different mouse lines. Scale bar, 100 μm. No specific staining was observed when a negative control probe (LNA-scramble) was used. (**c**) AFP mRNA expression in mouse liver tissues was analysed by quantitative RT-PCR. Data represent the mean±s.d. of results for five mice in each group. $^*P<0.05$ (*t*-test). (**d**) CUX1 and ZBTB20 expression in mouse liver tissues was assessed by Western blotting. A representative result from three independent experiments is shown. (**e**) Levels of miR214 in liver tissues were determined by quantitative RT-PCR. Data represent the mean±s.d. of three independent experiments. $^*P<0.05$ (*t*-test). (**f**) Protocols of the orthotopic xenograft models of HCC cells. Control and miR122-silenced PLC/PRF/5 cells were prepared and injected under the capsule of the left-lobe of the nude mouse liver. Six mice were included in each group. At 4 weeks after transplantation, liver tissues were collected and sliced in series. Histological examination by H&E staining was performed to examine the tumour cell invasion status. (**g**) Representative liver histology images at 4 weeks after transplantation of tumour cells are shown. Whereas only the transplanted HCC cells beneath the capsule of the liver edge could be detected (arrow, upper left panel), neither intrahepatic metastasis nor vascular invasion was observed in the livers of mice transplanted with control cells. In contrast, vascular invasion by multiple tumour cells (arrow, upper right panel) was observed in mice transplanted with miR122-silenced cells. Scale bar, 500 μm. WT, wild type.

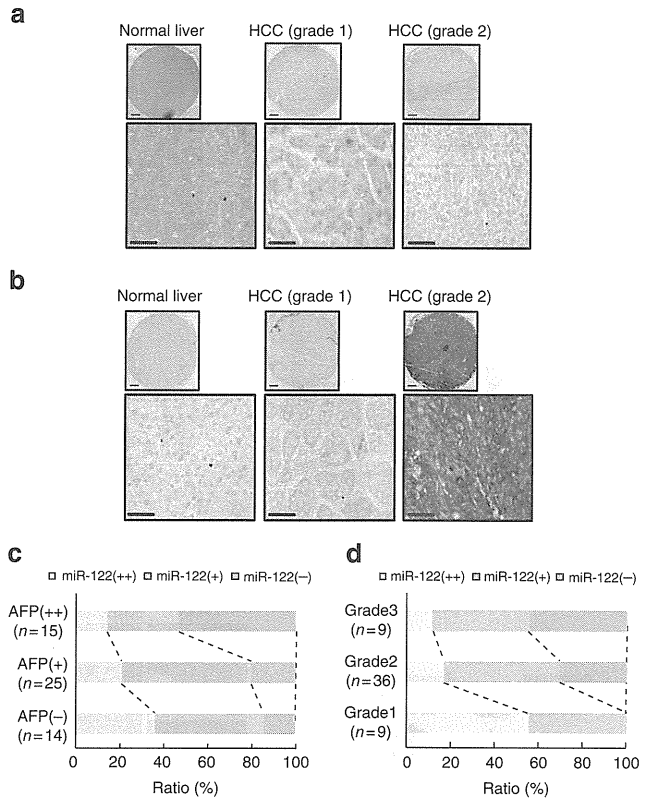

Figure 8 | AFP expression and HCC grade are inversely correlated with miR122 expression in human HCC samples. (**a**) Expression of miR122 in human clinical samples was assessed by *in situ* hybridization. Expression of miR122 (blue/purple staining) in grade 2 (more malignant) HCC samples was less than that of normal human liver tissues or grade 1 (less malignant) HCC samples. Representative images are shown. Nuclei were stained with FastRed. Scale bar, 500 μm. (**b**) AFP expression, shown in brown, was analysed by immunohistochemistry. AFP expression was higher in grade 2 HCC samples than in normal human liver tissue or grade 1 HCC samples in most cases. Representative images are shown. Scale bar, 500 μm. (**c**) Graph shows the correlation between miR122 and AFP expression. Increased AFP expression was correlated with decreased miR122 expression. (**d**) Graph shows the correlation between miR122 expression and malignancy grading of HCC. Increases in malignancy grading were correlated with decreases in miR122 expression.

are frequently observed simultaneously in the clinic: elevated expression of AFP and a more malignant biological phenotype. First, elevated AFP expression and greater cellular invasiveness were observed in miR122-knockdown cells *in vitro* and *in vivo*. Second, CUX1, which is linked with invasive characteristics in carcinoma cells[32,36,37], was shown to be involved in regulation of AFP expression and was identified as a direct target of miR122. Third, in human tissue samples from HCC patients, inverse correlations were observed between miR122 expression and AFP expression, and between miR122 expression and tumour grade. These data suggest that it is unlikely that the clinical correlation between elevated AFP levels and a more biologically aggressive phenotype in HCC is a coincidental epiphenomenon, but, instead provide a possible molecular explanation for the decrease in miR122 expression in HCC cells.

A recent study on liver development reported that liver-enriched transcription factors activate the expression of miR122, which in turn was found to promote terminal differentiation of hepatocytes through the silencing of CUX1 (ref. 42). In the present study, we confirmed that CUX1 is a direct target of miR122 and, in contrast to the situation in normal development, we showed that in grade 2 HCCs the decrease in miR122 is associated with higher CUX1 expression. High CUX1 expression was previously shown to inversely correlate with relapse-free and overall survival in high-grade breast cancers[36]. In transgenic mice, CUX1 was reported to cause various cancer-associated disorders depending on the specific isoform and tissue type expression[34,43–46]. In particular, expression of CUX1 caused organomegaly in several organs including the liver[43]. Hepatomegaly was associated with progression of lesions beginning with inflammation and leading to the development of mixed cell foci, hyperplasia and even HCCs, although in this last case statistical significance was not achieved because of the small size of the transgenic cohort[47]. The underlying mechanisms for the role of CUX1 in cancer is complex and is likely to involve both cell-autonomous and non-cell autonomous effects. However, from cell-based assays it is clear that CUX1 has a role in at least three distinct processes: cell motility, cell cycle progression and chromosome segregation[30,31,36,48]. The knockdown of CUX1 using siRNA was shown to delay entry into S phase and to hinder cell motility and invasion[31,36,48]. In contrast, overexpression of p110 CUX1 was able to accelerate S phase entry and to stimulate proliferation, migration and invasion[35,48]. Moreover, CUX1 was shown to promote genomic instability following cytokinesis failure[30]

Regulation of AFP gene expression is a complex process mediated by a number of transcriptional activators and repressors that bind the AFP gene[7,8]. ZBTB20 was recently identified as a potent repressor of AFP transcription in knockout mouse studies[9]. Our results demonstrate that decreased miR122 expression leads to concomitant decreases in ZBTB20 protein expression. This effect is mediated through upregulation of CUX1, as CUX1 silencing in miR122-silenced cells was shown to lead to both recovery of ZBTB20 levels and reduced AFP expression. Furthermore, the increased expression level of ZBTB20 in CUX1 knockdown cells suggests that ZBTB20 expression is regulated by CUX1. This miR122/CUX1/miR214/ZBTB20/AFP pathway may explain the deregulated AFP expression observed in HCC cells. Additionally, the ability of CUX1 to activate RhoA and to regulate the expression of many proteins involved in cell motility may explain the increased migration and invasiveness associated with malignancy of HCC[31–36]. It should be noted that, although this analysis revealed a trend toward inverse correlation between expression of miR122 and expression of AFP, this correlation could not be applied to all cases examined. Therefore, the possibility of additional pathways that regulate AFP expression cannot be discounted. Nonetheless, our results demonstrate that a decrease in miR122 function is a key factor that contributes to the regulation of AFP expression in HCC.

MiR122 is the most abundant miRNA in the normal adult liver, comprising approximately 80% of all miRNAs[18]. The numerous reported roles of miR122 include regulation of cholesterol biosynthesis[19,20], hepatitis C virus replication[49] and maintenance of the adult liver phenotype[21]. Specific miRNAs are often involved in the differentiation of specific cells and tissues[50]. As miR122 is liver-specific, we reasoned that this miRNA may have a role in the differentiation of normal hepatocytes. In our study, transgenic mice in which miR122 was functionally silenced were found to exhibit elevated AFP levels, but did not display abnormal morphological development in the liver (at least, not up to the age of 12 weeks), suggesting that decreased miR122 expression itself does not cause cells to become transformed. Ongoing characterization of these mice will be required to fully determine the physiological roles of miR122 in the noncancerous liver *in vivo*.

In summary, we have shown that decreased miR122 expression in HCC is linked both to more biologically aggressive tumour behaviour and elevated AFP expression. Furthermore, both of these effects were shown to be mediated by increased expression of CUX1, a direct target of miR122. Similar strategies could also be used to develop new therapeutics and diagnostics for other cancers in which miRNAs that regulate both tumour characteristics and serum markers have been identified.

Methods

Cell culture. The human HCC cell lines, Huh7, PLC/PRF/5, HepG2, Hep3B and Huh1 were obtained from the Japanese Collection of Research Bioresources. The human embryonic kidney cell line, 293T and the human breast cancer cell line HS578T were obtained from the American Type Culture Collection . All cells were maintained in Dulbecco's modified Eagle medium, supplemented with 10% fetal bovine serum.

Mouse experiments. All experiments were carried out in compliance with the regulations of the Animal Use Committee of The University of Tokyo and The Institute for Adult Disease, Asahi Life Foundation.

Generation of transgenic mice in which miR122 was functionally silenced. Mice in which miR122 function was knocked down were generated using previously described protocols[38,51]. Briefly, a DNA fragment of 1,085 bp, containing the H1 promoter region, the coding region for the antisense miR122 stem-loop-stem RNA precursor, and a transcriptional terminator of five thymidines, was resected from the miRZip-122 construct described above by digestion with *Pvu*II. Proper silencing function of the resulting DNA was confirmed via transient transfection-based reporter assays that showed efficient knockdown of miR122 function. Stable C57BL/6 embryonic stem cell lines were generated by electroporation of the linearized transgene, and the resulting cells were injected into blastocysts by the UNITECH Company. Genotyping was performed by PCR using DNA isolated from tail snips. Four different mouse lines were maintained and the male littermates were used in experiments.

Chromatin immunoprecipitation assay. ChIP for CUX1 was performed as previously described[52]. For the scanning ChIP of the miR214 locus, realtime PCR analysis was performed using primer pairs specific for different regions of the promoters. Templates for the PCR reactions were 0.1% total input DNA (I), nonspecific DNA from sepharose beads alone (S), or chipped chromatin. The respective fold enrichment of the different DNA fragments are indicated relative to the DNA obtained by purification on sepharose beads without IgG (S). Enrichment was calculated using the HPRT locus as a reference.

Doxycyclin-induced shRNA against CUX1 system. For conditional knockdown of CUX1 in Hs578t cells, we took advantage of the Addgene plasmid 11643. HS578T cells were infected with pLVCT shCUX1(5,326–5,348)-tTRKRAB lentivirus as described[53]. At 48 h after infection, cells were split and cultured with or without doxycyclin at a final concentration of 2.5 $\mu g\,ml^{-1}$. Cells were used for experiments after 5 days of treatment. Doxycyclin was then removed from the culture media and cells were maintained for 4 days following release.

Cell proliferation assay. Relative cell proliferation was assessed using a Cell Counting Kit-8 (Dojindo Laboratories), as described previously[54].

Enzyme-linked immunosorbent assay. AFP levels in the cell-culture supernatant were examined using an AFP-specific ELISA kit supplied by an outsourcing company, SRL.

Western blot analysis. Protein lysates were prepared from cells or mouse liver for immunoblot analysis. Proteins were separated by SDS–polyacrylamide gel electrophoresis and transferred to polyvinylidene difluoride membranes. After blocking with 5% dry milk to decrease nonspecific binding, membranes were probed with the appropriate primary antibodies. Primary antibodies were obtained from Abcam (ZBTB20, #ab48889, 1:500) and Santa Cruz Biotechnology (CDP, #sc-13024, 1:1,000). CUX1 antibodies (#861, 1:1,000) were generated as described previously[52]. Horseradish peroxidase-conjugated secondary antibodies were used to detect primary antibodies. Bound antibodies were detected using ECL Plus Western blotting detection reagents (GE Healthcare Life Sciences).

Scratch assay. The effects of miR122 knockdown on cellular migratory function were determined by evaluating cellular migration after scratching of a confluent monolayer of cells. Monolayers were cultured on 10 $\mu g\,ml^{-1}$ fibronectin-coated dishes and were scratched using a 200-µl pipette. Migration was analysed at the indicated time points after scratching.

***In vitro* invasion assay**. The effect of miR122 knockdown on invasive function was determined using BD BioCoat Matrigel Invasion Chambers (Becton Dickinson) according to the manufacturer's recommended protocol. Cell invasion was induced by removing the serum in the upper chamber. The number of invading cells was analysed after 22-h incubation. Cell numbers were counted in four randomly chosen fields at each time point.

Quantitative pseudopodia assay. Pseudopodium quantitation was performed using a Quantitative Pseudopodia Assay Kit (Chemicon) according to the manufacturer's instructions. Briefly, the upper chamber was coated with fibronectin and seeded with cells in serum-free medium. Serum was added to the lower chambers. 8 h later, pseudopodia on the lower surface were stained and eluted, and the absorbances of solubilized samples at 600 nm was measured using a microplate reader.

CUX1-knockdown lentiviral construct. Lentiviral particles expressing CUX1 shRNA were purchased from Santa Cruz Biotechnology (#sc-35051-V).

***In situ* hybridization to assess miR122 and miR214**. The expression of miR122 and miR214 in mouse liver and human HCC tissues was examined by *in situ* hybridization[55,56]. Locked nucleic acid (LNA)-scramble (negative control) and LNA-anti-miR122 and LNA-anti-miR214 probes were obtained from EXIQON. After deparaffinization, tissue sections were treated with 10 $\mu g\,ml^{-1}$ proteinase K for 5 min at 37 °C and refixed with 4% paraformaldehyde, followed by acetylation with 0.25% anhydrous acetic acid in 0.1 M Tris–HCl buffer (pH 8.0). Following pre-hybridization for 30 min at 48 °C, hybridization was performed overnight with each 20 nM LNA probe in hybridization buffer (5xSSC buffer, 50% formamide, 500 $\mu g\,ml^{-1}$ tRNA, 50 $\mu g\,ml^{-1}$ Cot-1 DNA). After completion of hybridization, the sections were washed with 0.1×SSC buffer for 10 min at 52 °C three times and blocked with DIG blocking buffer (Roche Diagnostics) for 30 min. Sections were then probed with anti-DIG (1:500; Roche Diagnostics) for 1 h at room temperature. Detection was performed by incubation in NBT/BCIP buffer (Promega) overnight. Nuclei were stained with Nuclear FastRed (Sigma-Aldrich).

Immunohistochemistry. Tissue arrays containing HCC tissues were purchased from US Biomax. To determine the correlations between AFP, ZBTB20, CUX1, miR122 and miR214 expression and HCC differentiation grade, slides carrying consecutive sections were obtained. Slides were baked at 65 °C for 1 h and deparaffinized. Endogenous peroxidase activity was blocked by incubation in 3% hydrogen peroxide buffer for 30 min. Antigen retrieval was performed by incubating the slides at 89 °C in 10 mM sodium citrate buffer (pH 6.0) for 30 min. To minimize nonspecific background staining, slides were blocked in 5% normal goat serum (Dako) for 10 min at room temperature. Tissues were labelled overnight at 4 °C with primary antibodies raised against AFP (Dako, #N1501, 1:100), CUX1 (#sc-13024, 1:100) and ZBTB20 (HPA016815, Sigma-Aldrich, 1:100). Slides were then incubated with anti-rabbit horseradish peroxidase-conjugated secondary antibodies (Nichirei Bioscience) for 1 h. Primary antibody binding was visualized by incubation in 3,3′-diaminobenzidine in buffered substrate (Nichirei Bioscience) for 5 min. The slides were counterstained with haematoxylin, dehydrated with ethanol, and mounted with Clarion mounting medium (Biomeda).

GTP-binding RhoA and Rac1 immunoprecipitation assay. The amount of RhoA activity was examined using an Active Rho Pull-down and Detection Kit (Thermo Fisher Scientific) according to the manufacturer's recommended protocol. The amount of GTP-bound RhoA protein (the active form of RhoA) was detected by Western blotting with the provided anti-RhoA antibody (1:100). Rac1 activity was similarly determined by using PAK-GST Protein Beads (#PAK02, Cytoskeleton) for pulldowns and anti-Rac1 antibodies (1:100) for subsequent Western blotting (#89856D, Thermo Fisher Scientific).

Orthotopic xenograft tumour model of HCC. Male BALB/c (nu/nu) nude mice were purchased from CREA Japan (Tokyo, Japan). The transplantation of tumour cells into mouse livers was performed using previously reported methods[57,58]. Briefly, 2×10^6 control or miR122-silenced PLC/PRF5 cells were suspended in 30 µl of PBS containing 1% Matrigel (Becton Dickinson). After anaesthesia, the liver was exposed through a surgical incision. Cells were slowly injected under the capsule of left lobe of the liver using a 28-gauge needle. When successful, a transparent bleb of cells could be seen through the liver capsule. After injection, light pressure was applied to the injection site with sterile gauze for 2 min to prevent bleeding and tumour cell leakage. The abdomen was then closed with sutures. Transplantation was successful in a total of 12 mice (6/group). At 4 weeks post-transplantation, liver tissues were collected, serially sectioned, and stained with haematoxylin and eosin.

Statistical analysis. Statistically significant differences between groups were determined using Student's *t*-test when variances were equal. When variances were unequal, Welch's *t*-test was used instead. *P*-values less than 0.05 were considered statistically significant.

Plasmid and stable cell line construction, reporter assays, RT–PCR, northern blotting and immunocytochemistry are described in the Supplementary Methods. All primer information is provided in Supplementary Table S1.

References

1. Parkin, D., Bray, F., Ferlay, J. & Pisani, P. Global cancer statistics, 2002. *CA Cancer J. Clin.* **55,** 74–108 (2005).
2. El-Serag, H. Epidemiology of hepatocellular carcinoma in USA. *Hepatol. Res.* **37,** S88–94 (2007).
3. Llovet, J. *et al.* Sorafenib in advanced hepatocellular carcinoma. *N. Engl. J. Med.* **359,** 378–390 (2008).
4. Greten, T. *et al.* Survival rate in patients with hepatocellular carcinoma: a retrospective analysis of 389 patients. *Br. J. Cancer* **92,** 1862–1868 (2005).
5. Greten, T., Korangy, F., Manns, M. & Malek, N. Molecular therapy for the treatment of hepatocellular carcinoma. *Br. J. Cancer* **100,** 19–23 (2009).
6. Di Bisceglie, A. Issues in screening and surveillance for hepatocellular carcinoma. *Gastroenterology* **127,** S104–S107 (2004).

7. Ogden, S. *et al. p53* targets chromatin structure alteration to repress alpha-fetoprotein gene expression. *J. Biol. Chem.* **276,** 42057–42062 (2001).
8. Peng, S. *et al.* High alpha-fetoprotein level correlates with high stage, early recurrence and poor prognosis of hepatocellular carcinoma: significance of hepatitis virus infection, age, p53 and beta-catenin mutations. *Int. J. Cancer.* **112,** 44–50 (2004).
9. Xie, Z. *et al.* Zinc finger protein ZBTB20 is a key repressor of alpha-fetoprotein gene transcription in liver. *Proc. Natl Acad. Sci. USA* **105,** 10859–10864 (2008).
10. Oishi, K. *et al.* Clinicopathologic features of poorly differentiated hepatocellular carcinoma. *J. Surg. Oncol.* **95,** 311–316 (2007).
11. Yamamoto, K. *et al.* AFP, AFP-L3, DCP, and GP73 as markers for monitoring treatment response and recurrence and as surrogate markers of clinicopathological variables of HCC. *J. Gastroenterol.* **45,** 1272–1282 (2010).
12. Matsumoto, Y. *et al.* Clinical classification of hepatoma in Japan according to serial changes in serum alpha-fetoprotein levels. *Cancer* **49,** 354–360 (1982).
13. Lee, R., Feinbaum, R. & Ambros, V. The *C. elegans* heterochronic gene lin-4 encodes small RNAs with antisense complementarity to lin-14. *Cell* **75,** 843–854 (1993).
14. Carrington, J. & Ambros, V. Role of microRNAs in plant and animal development. *Science* **301,** 336–338 (2003).
15. Bartel, D. MicroRNAs: genomics, biogenesis, mechanism, and function. *Cell* **116,** 281–297 (2004).
16. Ambros, V. The functions of animal microRNAs. *Nature* **431,** 350–355 (2004).
17. Lu, J. *et al.* MicroRNA expression profiles classify human cancers. *Nature* **435,** 834–838 (2005).
18. Landgraf, P. *et al.* A mammalian microRNA expression atlas based on small RNA library sequencing. *Cell* **129,** 1401–1414 (2007).
19. Krützfeldt, J. *et al.* Silencing of microRNAs *in vivo* with 'antagomirs'. *Nature* **438,** 685–689 (2005).
20. Esau, C. *et al.* miR-122 regulation of lipid metabolism revealed by *in vivo* antisense targeting. *Cell Metab.* **3,** 87–98 (2006).
21. Gatfield, D. *et al.* Integration of microRNA miR-122 in hepatic circadian gene expression. *Genes Dev.* **23,** 1313–1326 (2009).
22. Yan, D. *et al.* MicroRNA-1/206 targets c-Met and inhibits rhabdomyosarcoma development. *J. Biol. Chem.* **284,** 29596–29604 (2009).
23. Kutay, H. *et al.* Downregulation of miR-122 in the rodent and human hepatocellular carcinomas. *J. Cell. Biochem.* **99,** 671–678 (2006).
24. Coulouarn, C., Factor, V., Andersen, J., Durkin, M. & Thorgeirsson, S. Loss of miR-122 expression in liver cancer correlates with suppression of the hepatic phenotype and gain of metastatic properties. *Oncogene* **28,** 3526–3536 (2009).
25. Tsai, W. *et al.* MicroRNA-122 a tumor suppressor microRNA that regulates intra-hepatic metastasis of hepatocellular carcinoma. *Hepatology* **49,** 1571–1582 (2009).
26. Varnholt, H. *et al.* MicroRNA gene expression profile of hepatitis C virus-associated hepatocellular carcinoma. *Hepatology* **47,** 1223–1232 (2008).
27. Wong, Q. *et al.* MicroRNA-223 is commonly repressed in hepatocellular carcinoma and potentiates expression of Stathmin1. *Gastroenterology* **135,** 257–269 (2008).
28. Sahai, E. & Marshall, C. RHO-GTPases and cancer. *Nat. Rev. Cancer* **2,** 133–142 (2002).
29. Sansregret, L. & Nepveu, A. The multiple roles of CUX1: insights from mouse models and cell-based assays. *Gene* **412,** 84–94 (2008).
30. Sansregret, L. *et al.* Cut homeobox 1 causes chromosomal instability by promoting bipolar division after cytokinesis failure. *Proc. Natl Acad. Sci. USA* **108,** 1949–1954 (2011).
31. Kedinger, V. & Nepveu1, A. The roles of CUX1 homeodomain proteins in the establishment of a transcriptional program required for cell migration and invasion. *Cell Adh. Migr.* **4,** 348–352 (2010).
32. Michl, P., Knobel, B. & Downward, J. CUTL1 is phosphorylated by protein kinase A, modulating its effects on cell proliferation and motility. *J. Biol. Chem.* **281,** 15138–15144 (2006).
33. Seguin, L. *et al.* CUX1 and E2F1 regulate coordinated expression of the mitotic complex genes Ect2, MgcRacGAP, and MKLP1 in S phase. *Mol. Cell Biol.* **29,** 570–581 (2009).
34. Kedinger, V. *et al.* p110 CUX1 homeodomain protein stimulates cell migration and invasion in part through a regulatory cascade culminating in the repression of E-cadherin and occludin. *J. Biol. Chem.* **284,** 27701–27711 (2009).
35. Michl, P. *et al.* CUTL1 is a target of TGF(beta) signaling that enhances cancer cell motility and invasiveness. *Cancer Cell* **7,** 521–532 (2005).
36. Aleksic, T. *et al.* CUTL1 promotes tumor cell migration by decreasing proteasome-mediated Src degradation. *Oncogene* **26,** 5939–5949 (2007).
37. Kunath, T. *et al.* Transgenic RNA interference in ES cell-derived embryos recapitulates a genetic null phenotype. *Nat. Biotechnol.* **21,** 559–561 (2003).
38. Shouval, D. *et al.* Tumorigenicity in nude mice of a human hepatoma cell line containing hepatitis B virus DNA. *Cancer Res.* **41,** 1342–1350 (1981).
39. Nomura, F., Ohnishi, K. & Tanabe, Y. Clinical features and prognosis of hepatocellular carcinoma with reference to serum alpha-fetoprotein levels. Analysis of 606 patients. *Cancer* **64,** 1700–1707 (1989).
40. Johnson, P., Melia, W., Palmer, M., Portmann, B. & Williams, R. Relationship between serum alpha-foetoprotein, cirrhosis and survival in hepatocellular carcinoma. *Br. J. Cancer* **44,** 502–505 (1981).
41. Xu, H. *et al.* Liver-enriched transcription factors regulate microRNA-122 that targets CUTL1 during liver development. *Hepatology* **52,** 1431–1442 (2010).
42. Ledford, A. W. *et al.* Deregulated expression of the homeobox gene Cux-1 in transgenic mice results in downregulation of p27(kip1) expression during nephrogenesis, glomerular abnormalities, and multiorgan hyperplasia. *Dev. Biol.* **245,** 157–171 (2002).
43. Brantley, J. G., Sharma, M., Alcalay, N. I. & Heuvel, G. B. Cux-1 transgenic mice develop glomerulosclerosis and interstitial fibrosis. *Kidney Int.* **63,** 1240–1248 (2003).
44. Cadieux, C. *et al.* Mouse mammary tumor virus p75 and p110 CUX1 transgenic mice develop mammary tumors of various histologic types. *Cancer Res.* **69,** 7188–7197 (2009).
45. Cadieux, C. *et al.* Polycystic kidneys caused by sustained expression of Cux1 isoform p75. *J. Biol. Chem.* **283,** 13817–13824 (2008).
46. Cadieux, C. *et al.* Transgenic mice expressing the p75 CCAAT-displacement protein/Cut homeobox isoform develop a myeloproliferative disease-like myeloid leukemia. *Cancer Res.* **66,** 9492–9501 (2006).
47. Vanden Heuvel, G. B. *et al.* Hepatomegaly in transgenic mice expressing the homeobox gene Cux-1. *Mol. Carcinog.* **43,** 18–30 (2005).
48. Sansregret, L. *et al.* The p110 isoform of the CDP/Cux transcription factor accelerates entry into S phase. *Mol. Cell Biol.* **26,** 2441–2455 (2006).
49. Jopling, C., Yi, M., Lancaster, A., Lemon, S. & Sarnow, P. Modulation of hepatitis C virus RNA abundance by a liver-specific MicroRNA. *Science* **309,** 1577–1581 (2005).
50. Taulli, R. *et al.* The muscle-specific microRNA miR-206 blocks human rhabdomyosarcoma growth in xenotransplanted mice by promoting myogenic differentiation. *J. Clin. Invest.* **119,** 2366–2378 (2009).
51. Zhou, Y. *et al.* Chimeric mouse tumor models reveal differences in pathway activation between ERBB family- and KRAS-dependent lung adenocarcinomas. *Nat. Biotechnol.* **28,** 71–78 (2010).
52. Harada, R. *et al.* Genome-wide location analysis and expression studies reveal a role for p110 CUX1 in the activation of DNA replication genes. *Nucleic Acids Res.* **36,** 189–202 (2008).
53. Szulc, J., Wiznerowicz, M., Sauvain, M. O., Trono, D. & Aebischer, P. A versatile tool for conditional gene expression and knockdown. *Nat. Methods* **3,** 109–116 (2006).
54. Maeda, S. *et al.* Ikappa B kinasebeta/nuclear factor-kappaB activation controls the development of liver metastasis by way of interleukin-6 expression. *Hepatology* **50,** 1851–1860 (2009).
55. Elmén, J. *et al.* LNA-mediated microRNA silencing in non-human primates. *Nature* **452,** 896–899 (2008).
56. Bai, S. *et al.* MicroRNA-122 inhibits tumorigenic properties of hepatocellular carcinoma cells and sensitizes these cells to sorafenib. *J. Biol. Chem.* **284,** 32015–32027 (2009).
57. Yao, X. *et al.* A novel orthotopic tumor model to study growth factors and oncogenes in hepatocarcinogenesis. *Clin. Cancer Res.* **9,** 2719–2726 (2003).
58. Kim, M. *et al.* Generation of orthotopic and heterotopic human pancreatic cancer xenografts in immunodeficient mice. *Nat. Protoc.* **4,** 1670–1680 (2009).

Acknowledgments

This work was supported by Grants-in-Aid from the Ministry of Education, Culture, Sports, Science and Technology, Japan (#22390058, #22590718, #17016016 and #20390204) (to M. Otsuka, Y. Kondo, M. Omata and K. Koike), by Health Sciences Research Grants of The Ministry of Health, Labour and Welfare of Japan (Research on Hepatitis) (to K. Koike), by grants from the Takeda Science Foundation, Astellas Foundation for Research on Metabolic Disorders, Senri Life Science Foundation, the Foundation for Promotion of Cancer Research and the Mochida Memorial Foundation for Medical and Pharmaceutical Research (to M. Otsuka), and by the grant 019389 from the Canadian Cancer Society (to A.N.).

Author contributions

K. Kojima, M. Otsuka and A.N. planned the research and wrote the paper. K. Kojima, A.T., C.V., T.Y., Y. Kondo, Y. Kang and Z.X. performed the majority of the experiments. M.A., N.K., W.Z. and A.N. contributed materials. T.K. and H.Y. supported several experiments. M. Omata and K. Koike supervised the entire project.

Additional information

Supplementary Information accompanies this paper at http://www.nature.com/naturecommunications

Competing financial interests: The authors declare no competing financial interests.

Reprints and permission information is available online at http://npg.nature.com/reprintsandpermissions/

How to cite this article: Kojima, K. *et al.* MiRNA122 is a key regulator of α-fetoprotein expression and influences the aggressiveness of hepatocellular carcinoma. *Nat. Commun.* 2:338 doi: 10.1038/ncomms1345 (2011).

Living Donor Liver Transplantations in HIV- and Hepatitis C Virus-Coinfected Hemophiliacs: Experience in a Single Center

Kunihisa Tsukada,[1,2] Yasuhiko Sugawara,[3,10] Junichi Kaneko,[3] Sumihito Tamura,[3] Natsuo Tachikawa,[2,4] Yuji Morisawa,[1,5] Shu Okugawa,[1] Yoshimi Kikuchi,[2] Shinichi Oka,[2] Satoshi Kimura,[1,2,6] Yutaka Yatomi,[7] Masatoshi Makuuchi,[8] Norihiro Kokudo,[3] and Kazuhiko Koike[1,9]

Background. Although almost all human immunodeficiency virus (HIV)-infected Japanese hemophiliacs are coinfected with hepatitis C virus (HCV), the outcome of living donor liver transplantation (LDLT) in such patients in terms of survival rate, perioperative complications, and recovery of coagulation activity is poorly understood.
Patients and Methods. Six HIV-positive hemophiliacs underwent LDLT for HCV-associated advanced cirrhosis. The mean CD4 T-cell count at transplantation was 376±227/μL.
Results. The 1-, 3-, and 5-year survival rates were 66%, 66%, and 50%, respectively. Fatal perioperative bleeding related to hemophilia was not observed. Two patients died within 6 months after transplantation due to graft failure. HIV infection was well controlled in all patients who survived longer than 6 months. Two patients (genotype 2a and 2+3a) achieved a sustained viral response and both of them were alive at the end of follow-up period, whereas one patient (genotype 1a+1b) died of decompensated cirrhosis 4 years after transplantation due to recurrent HCV infection.
Conclusions. HIV/HCV-coinfected hemophiliacs can safely undergo LDLT. Hemophilia was clinically cured after successful transplantation. A good outcome can be expected as long as postoperative hepatitis C is controlled with interferon/ribavirin combination therapy.

Keywords: Hepatitis C virus, Living donor liver transplantation, HIV, HAART.

(*Transplantation* 2011;91: 1261–1264)

Because of the availability of highly active antiretroviral therapy (HAART), the life expectancy of patients infected with human immunodeficiency virus (HIV) has dramatically improved (*1*). Death from opportunistic infections has decreased and, as the result, non-acquired immune deficiency syndrome (AIDS)-defining complications such as hepatic diseases, cardiovascular diseases, or non-AIDS malignancies have emerged as the most important problems (*2*, *3*).

Hepatitis C virus (HCV) and HIV often coinfect due to their shared route of transmission. A recent report indicated that approximately 20% of HIV-infected people in Japan are coinfected with HCV (*4*), a large proportion of whom are hemophiliacs. Approximately 1500 hemophiliacs were infected with HIV through non heat-treated concentrated coagulation factor administration between 1981 and 1985, and 98% of them were also infected with HCV. The coexistence of HIV infection with HCV accelerates the progression of liver fibrosis (*5*) and attenuates the efficacy of interferon (IFN) treatment for HCV (*6*, *7*). A considerable number of such coinfected patients suffer from decompensated cirrhosis or hepatocellular carcinoma (HCC) (*8*). In the HAART era, AIDS-related death is gradually decreasing (*9*) and HCV-

This work was supported by a Grant-in-aid for Scientific Research from the Ministry of Education, Culture, Sports, Science and Technology of Japan and from the Ministry of Health, Labor and Welfare of Japan (AIDS Research).

[1] Department of Infectious Diseases, Graduate School of Medicine, the University of Tokyo, Bunkyo-Ku, Tokyo.
[2] AIDS Clinical Center, National Center for Global Health and Medicine, Shinjuku-ku, Tokyo, Japan.
[3] Division of Artificial Organ and Transplantation, Department of Surgery, the University of Tokyo, Bunkyo-Ku, Tokyo.
[4] Yokohama Municipal Citizens Hospital, Yokohama, Japan.
[5] Department of Infection Control, Jichi Medical School, Tochigi-ken, Japan.
[6] Tokyo Teishin Hopital, Chiyoda-ku, Tokyo, Japan.
[7] Department of Clinical Laboratory Medicine, the University of Tokyo, Bunkyo-Ku, Tokyo.
[8] Japanese Red Cross Hospital, Shibuya-Ku, Tokyo, Japan.
[9] Department of Gastroenterology, Graduate School of Medicine, the University of Tokyo, Bunkyo-Ku, Tokyo.
[10] Address correspondence to: Yasuhiko Sugawara, M.D., Division of Artificial Organ and Transplantation, Department ofSurgery, University of Tokyo, 7-3-1 Hongo, Bunkyo-Ku, Tokyo.
E-mail: yasusugatky@yahoo.co.jp

K.T., Y.S., J.K., S.T., Y.Y., M.M., N.K., and K.K. participated in research design; K.T. and Y.S. participated in the writing of the manuscript; and N.T., Y.M., S.O., Y.K., S.O., and S.K. participated in the performance of the research.
Received 2 December 2010. Revision requested 3 January 2011.
Accepted 7 March 2011.

ISSN 0041-1337/11/9111-1261
DOI: 10.1097/TP.0b013e3182193cf3

related liver diseases have become the leading cause of death in Japanese hemophiliacs (*10*).

The only curative treatment for end-stage liver disease is liver transplantation. In the pre-HAART era, HIV infection was considered an absolute or relative contraindication for transplantation. Several cases were reported during that period (*11*, *12*), but the outcomes were not always satisfactory. In the HAART era, more than 50 cases of HIV-positive liver transplantation have been reported (*13–21*), and survival after liver transplantation seems to be more promising.

The absolute number of deceased donor livers in Japan is small, and living donor liver transplantation (LDLT) is the mainstay of liver transplantation. We reported the first LDLT in an HIV-positive hemophiliac in 2002 (*22*). Here, we present a series of six cases of LDLT in HIV/HCV-coinfected hemophiliacs performed at the University of Tokyo Hospital between 2001 and 2004.

RESULTS

Survival

The 1-, 3-, and 5-year survival rates were 66%, 66%, and 50%, respectively. Two patients (cases 2 and 5) died on postoperative day (POD) 99 and 156, respectively. The causes of early death were graft failure and bleeding from cytomegalovirus (CMV) enteritis (case 2) and graft failure suspected to be cholestatic hepatitis (case 5). One patient died 50 months after LDLT due to recurrent HCV-related cirrhosis.

Results of Antiviral Therapy for Recurrent Hepatitis C in the Graft

After LDLT, all but one (case 2) patients received combination therapy with IFN (standard or pegylated form) and ribavirin. Case 3 was treated for biopsy-proven recurrent hepatitis C, whereas the other four were treated preemptively (started on POD, 10–70 days). Duration of anti-HCV therapy was 12 months in case early viral response was achieved. Cases 1 and 3 achieved sustained viral response (SVR). Case 3 suffered from HCV-related cholestatic hepatitis on POD 38, which responded well to combination therapy with IFN and ribavirin and he eventually achieved SVR. The other patients did not achieve SVR. Cases 4 and 6 showed a biochemical response and were on maintenance antiviral therapy. In case 6, tacrolimus was switched to cyclosporine A 15 months after LDLT to suppress HCV replication. This lead to a transient 10-fold decrease in HCV-RNA, but it returned to the previous value within several months.

Results of Antiretroviral Therapy After LDLT

Antiretroviral therapy was transiently terminated during the perioperative period. The timing of reintroduction was individualized according to the CD4 count, HIV viral load, general status such as surgical complication and the result of liver function tests. One patient (case 1) has continued to maintain a high CD4 count without antiretroviral therapy. One patient (case 2) died before antiretroviral reintroduction.

The remaining four patients started antiretroviral therapy at a median of 56.5 days after LDLT (range, 43–485 days). The choice of the antiretroviral drug was individualized according to each patient's antiretroviral history and accumulated resistance mutations. A protease inhibitor-based combination was selected in all cases. All but one patient (case 5) tolerated antiretroviral therapy and had an excellent response. The blood concentration of the immunosuppressant increased drastically from the first day of protease inhibitor administration, which was controlled by close monitoring and dosage modification.

Elevation of serum alkaline-phosphatase and gamma-glutanyl-transpeptidase values was observed in all patients after antiretroviral reintroduction. Other significant adverse effects include severe allergic reaction to lamivudine (case 3) and liver failure, which was clinically diagnosed to be cholestatic hepatitis as an immune reconstitution inflammatory syndrome against HCV (case 5).

One patient (case 3) developed Burkitt leukemia 38 months after LDLT. His CD4 count at that time was 480/μL and HIV-RNA was undetectable. Combination chemotherapy using cyclophosphamide, vincristine, doxorubicin, and dexamethasone (*23*) was effective, and he eventually achieved complete remission. Other opportunistic infections included multiple abscess formation at the surgical site in two patients (case 2 by methicillin-resistant *Staphylococcus aureus* and case 5 by multi-drug resistant *Pseudomonas aeruginosa*). Positive CMV antigenemia was observed in all cases. However, only one patient (case 2) presented with clinically overt organ damage.

Restoration of Coagulation After LDLT

Except for case 5, replacement became unnecessary within 1 week after operation. In case 5, in addition to insufficient endogenous coagulation factor production, re-operation was necessary several times, and the coagulation factor replacement could not be withdrawn. Cases 2 and 6 again required coagulation factor replacement after graft failure became apparent.

Outcome of the Donors

All donors were alive without major complications at the point of analysis. Two donors were considered obligate carriers of hemophilia and one of them (donor of case 5) showed relatively low coagulation activity, but none of the donors experienced abnormal bleeding requiring coagulation factor administration. The donor of case 5 experienced transient decrease in factor IX activity after liver resection. However, the value of coagulation activity recovered without supplementation.

DISCUSSION

Recurrence of hepatitis C is the most important problem in treating HCV-positive hemophiliac patients. Recent reports indicate that HIV/HCV-coinfected liver recipients have a relatively lower survival rate than HCV-monoinfected liver recipients, although the difference is not significant. In our series, two of three deaths were related to recurrent HCV, and two patients experienced fibrosing cholestatic hepatitis. Cholestatic hepatitis is characterized by a high rate of HCV replication and a paucity of inflammatory activity, and the risk might increase in LDLT recipients (*24*, *25*). In our center, IFN therapy is usually introduced preemptively as soon as possible. In our series, two cases infected with non-1b virus achieved SVR, whereas others did not achieve SVR. A report demonstrated the effectiveness of maintenance therapy with

pegylated (PEG)-IFN plus ribavirin (*26*), but this efficacy was not apparent in our series. Combination antiviral therapy with protease and polymerase inhibitors may improve the treatment results in the future.

With regard to HIV infection, when to restart antiretroviral therapy after LDLT has remained a question. Hemophiliacs often have a long-term treatment history. Five of six cases had a multiple history of treatment failure, and as a result, only one or two reliable antiretroviral combinations were available to each patient in that era. Protease inhibitors, key drugs for successful HIV suppression in such cases have a potential risk of liver toxicity, especially in those with HCV coinfection (*27*). Unlike whole liver transplantation, the initial graft size is relatively small in LDLT. The graft gradually increases its volume within several weeks after transplantation, and an unfavorable effect of antiretroviral treatment on graft growth during this period is a concern. Moreover, unintended treatment interruption due to early phase complications may result in further accumulation of resistance-associated mutations. Taking these issues into account, we delayed starting antiretroviral therapy until at least 4 weeks after LDLT. It is obvious, however, that earlier antiretroviral reintroduction has more benefit toward reducing opportunistic infections and improving the result of anti-HCV therapy after LDLT. The effectiveness and safety of a new class antiretrovirals, raltegravir (*28*), and enfuvirtide (*29*), were recently reported, and these compounds may play an important role in the management of HIV-infected split-graft recipients.

In our series, the immunosuppressant trough level was targeted to the same level as that in HIV-negative cases. It is not known, however, whether HIV-infected patients, particularly those with a relatively lower CD4 cell count, need the same blood level of immunosuppressants. Moreover, the CD4 cell count, may not act as accurate surrogate marker for immune function in those taking an immunosuppressant or steroid. In case 2, recurrent bleeding from CMV intestinal ulcer eventually led to death after immunosuppression was intensified to treat severe graft rejection. In this case, antiretroviral therapy could not be reintroduced because of severe liver damage, which might enhance excess immunosuppression. A more precise indicator than CD4 count and immunosuppressant level is needed. Dose modification of immunosuppressive drugs using an immune function assay (*30*) may contribute to more precise management, especially in HIV-coinfected patients.

A considerable number of HIV/HCV-coinfected patients are suffering from decompensated cirrhosis or HCC (*8*), and some of them are potential candidates for future liver transplantation. The shortage of deceased donor liver grafts is a major problem worldwide. LDLT can overcome such a problem. Clearly, regenerative medicine will have an important role in this field in the future. Those patients who are already in a cirrhotic state, however, cannot wait for such an innovative modality to be established. In our series, all patients who tolerated antiretroviral therapy achieved good HIV control, and those who cleared HCV survived long. Clinical cure of hemophilia after successful transplantation drastically improved the patients' quality of life. Cure of hemophilia also lead to considerable cost reduction. LDLT continues to have an important role in HIV-infected hemophiliacs.

MATERIALS AND METHODS

From April 2001 to October 2004, nine HIV/HCV-coinfected patients were referred to the University of Tokyo hospital for LDLT. The indication was HCV-related end-stage liver disease.

HIV-positive patients should meet the same standard criteria for liver transplantation as HIV-negative patients. The criteria for accepting candidates for LDLT were absolute CD4 T lymphocyte count more than 200/μL, or more than 14% CD4 proportion to total lymphocytes when hypersplenism-related leukocytopenia was considered the cause of an apparent decrease in the CD4 count. Undetectable HIV RNA was not required as long as effective HIV suppression was expected after transplantation. Exclusion criteria related to HIV infection were active AIDS-defining diseases except for esophageal candidiasis. All cases were approved by the ethics committee at the University of Tokyo. Donor was selected from those with spontaneous will and within the third-degree consanguinity of the patient. Those with abnormal coagulation values were excluded from candidate for the donor.

Two patients did not meet the criteria (one with concomitant uncontrollable fungal infection and one without appropriate donor). One patient retracted consent before operation. Finally, six HIV/HCV-coinfected hemophiliacs underwent LDLT. Two patients were transplanted emergently (within 2 weeks after referral) because of progressive hepatic encephalopathy and hepatorenal syndrome. None of the patients had concomitant active hepatitis B, HCC, or other malignancies. The patient characteristics are summarized in Table 1.

The appropriate type of concentrated coagulation factor was administered during the perioperative period. Concentrated coagulation factor was administered as a bolus just before the operation to achieve 100% coagulating

TABLE 1. Patient characteristics at LDLT and outcome

Case	Age/ sex	Type of hemophilia	HCV genotype	HCV-RNA at LDLT (KIU/mL)	HIV load (copy/mL)	MELD at LDLT	CCr	HTN/ DM	BMI	Graft	Graft size (%SLV)	ACR	CMV	Survival (mo)	Donor
1	41M	B	2a	3	UD	23	24	N/N	19.1	Right	66	0	1	Alive (115)	Brother
2	28M	A	2a, 2b	1410	6.2×10^4	15	76	N/N	23.4	Right	57	2	2	Died (3)	Mother
3	30M	A	1b, 3a	740	3.2×10^4	15	78	N/N	21.5	Right	42	1	2	Alive (96)	Mother
4	38M	A	1b, 3a	200	UD	34	69	N/N	20.0	Right	47	1	1	Alive (82)	Sister
5	31M	B	1a	747	2.6×10^4	18	72	N/N	24.3	Right	47	2	3	Died (5)	Mother
6	32M	B	1a, 1b	41	UD	48	62	N/N	25.2	Right	63	0	0	Died (50)	Father

HCV, hepatitis C virus; LDLT, living donor liver transplantation; HIV, human immunodeficiency virus; MELD, model for end-stage liver disease; CCr, creatine clearance; HTN, hypertension; DM, diabetes mellitus; BMI, body mass index; SLV, standard liver volume; ACR, acute cellular rejection; CMV, cytomegalovirus; UD, undetectable.

factor activity, followed by continuous infusion to maintain greater than 80% activity during the operation. Fresh-frozen plasma was also replaced. Initial dosage of the coagulation factor was calculated based on the results of preoperative pharmacokinetic studies, and the rate of continuous infusion was adjusted as necessary by periodical monitoring of coagulation factor activity.

Tacrolimus and steroids based immunosuppression was planned as previously described (*31*). The target tacrolimus trough level was same as that for the HIV-negative population. Moderate to severe rejection was treated with pulse steroids±mycophenolate mofetil.

The preoperative HCV-RNA value was positive in all subjects. The HCV genotype is listed in Table 1. All patients underwent concomitant splenectomy (*32*). Preemptive anti-HCV therapy with IFN (standard or pegylated form) plus ribavirin was planned after LDLT (*33*). Postoperative CMV reactivation was monitored using a pp65 antigen detecting method (CMV antigenemia), and a positive result was preemptively treated with ganciclovir (*34*) or valganciclovir.

ACKNOWLEDGMENTS

The authors thank Dr. Fukutake, Department of Laboratory Medicine, Tokyo Medical School, and Drs. Kusama and Nakajima at the Pharmaceutical Department in the University of Tokyo Hospital for technical support of perioperative coagulation management.

REFERENCES

1. Mocroft A, Ledergerber B, Katlama C, et al. Decline in the AIDS and death rates in the EuroSIDA study: An observational study. *Lancet* 2003; 362: 22.
2. Palella FJ Jr, Baker RK, Moorman AC, et al. Mortality in the highly active antiretroviral therapy era: Changing causes of death and disease in the HIV outpatient study. *J Acquir Immune Defic Syndr* 2006; 43: 27.
3. Weber R, Sabin CA, Friis-Moller N, et al. Liver-related deaths in persons infected with the human immunodeficiency virus: The D:A:D study. *Arch Intern Med* 2006; 166: 1632.
4. Koike K, Tsukada K, Yotsuyanagi H, et al. Prevalence of coinfection with human immunodeficiency virus and hepatitis C virus in Japan. *Hepatol Res* 2007; 37: 2.
5. Mohsen AH, Easterbrook PJ, Taylor C, et al. Impact of human immunodeficiency virus (HIV) infection on the progression of liver fibrosis in hepatitis C virus infected patients. *Gut* 2003; 52: 1035.
6. Chung RT, Andersen J, Volberding P, et al. Peginterferon alfa-2a plus ribavirin versus interferon alfa-2a plus ribavirin for chronic hepatitis C in HIV-coinfected persons. *N Engl J Med* 2004; 351: 451.
7. Torriani FJ, Rodriguez-Torres M, Rockstroh JK, et al. Peginterferon Alfa-2a plus ribavirin for chronic hepatitis C virus infection in HIV-infected patients. *N Engl J Med* 2004; 351: 438.
8. Yotsuyanagi H, Kikuchi Y, Tsukada K, et al. Chronic hepatitis C in patients co-infected with human immunodeficiency virus in Japan: A retrospective multicenter analysis. *Hepatol Res* 2009; 39: 657.
9. Tatsunami S, Fukutake K, Taki M, et al. Observed decline in the rate of death among Japanese hemophiliacs infected with HIV-1. *Int J Hematol* 2000; 72: 256.
10. Tatsunami S, Taki M, Shirahata A, et al. Increasing incidence of critical liver disease among causes of death in Japanese hemophiliacs with HIV-1. *Acta Haematol* 2004; 111: 181.
11. Tzakis AG, Cooper MH, Dummer JS, et al. Transplantation in HIV+ patients. *Transplantation* 1990; 49: 354.
12. Gordon FH, Mistry PK, Sabin CA, et al. Outcome of orthotopic liver transplantation in patients with haemophilia. *Gut* 1998; 42: 744.
13. Moreno-Cuerda VJ, Morales-Conejo M. Liver transplantation in patients with HIV infection. *Gastroenterol Hepatol* 2005; 28: 258.
14. Neff GW, Bonham A, Tzakis AG, et al. Orthotopic liver transplantation in patients with human immunodeficiency virus and end-stage liver disease. *Liver Transpl* 2003; 9: 239.
15. Norris S, Taylor C, Muiesan P, et al. Outcomes of liver transplantation in HIV-infected individuals: The impact of HCV and HBV infection. *Liver Transpl* 2004; 10: 1271.
16. Fung J, Eghtesad B, Patel-Tom K, et al. Liver transplantation in patients with HIV infection. *Liver Transpl* 2004; 10: S39.
17. Vogel M, Voigt E, Schafer N, et al. Orthotopic liver transplantation in human immunodeficiency virus (HIV)-positive patients: Outcome of 7 patients from the Bonn cohort. *Liver Transpl* 2005; 11: 1515.
18. Roland ME, Stock PG. Liver transplantation in HIV-infected recipients. *Semin Liver Dis* 2006; 26: 273.
19. Mindikoglu AL, Regev A, Magder LS. Impact of human immunodeficiency virus on survival after liver transplantation: Analysis of United Network for Organ Sharing database. *Transplantation* 2008; 85: 359.
20. Tateo M, Roque-Afonso AM, Antonini TM, et al. Long-term follow-up of liver transplanted HIV/hepatitis B virus coinfected patients: Perfect control of hepatitis B virus replication and absence of mitochondrial toxicity. *AIDS* 2009; 23: 1069.
21. Testillano M, Fernandez JR, Suarez MJ, et al. Survival and hepatitis C virus recurrence after liver transplantation in HIV- and hepatitis C virus-coinfected patients: Experience in a single center. *Transplant Proc* 2009; 41: 1041.
22. Sugawara Y, Ohkubo T, Makuuchi M, et al. Living-donor liver transplantation in an HIV-positive patient with hemophilia. *Transplantation* 2002; 74: 1655.
23. Cortes J, Thomas D, Rios A, et al. Hyperfractionated cyclophosphamide, vincristine, doxorubicin, and dexamethasone and highly active antiretroviral therapy for patients with acquired immunodeficiency syndrome-related Burkitt lymphoma/leukemia. *Cancer* 2002; 94: 1492.
24. Troppmann C, Rossaro L, Perez RV, et al. Early, rapidly progressive cholestatic hepatitis C reinfection and graft loss after adult living donor liver transplantation. *Am J Transplant* 2003; 3: 239.
25. Gaglio PJ, Malireddy S, Levitt BS, et al. Increased risk of cholestatic hepatitis C in recipients of grafts from living versus cadaveric liver donors. *Liver Transpl* 2003; 9: 1028.
26. Kornberg A, Kupper B, Tannapfel A, et al. Antiviral maintenance treatment with interferon and ribavirin for recurrent hepatitis C after liver transplantation: Pilot study. *J Gastroenterol Hepatol* 2007; 22: 2135.
27. Sulkowski MS. Drug-induced liver injury associated with antiretroviral therapy that includes HIV-1 protease inhibitors. *Clin Infect Dis* 2004; 38: S90.
28. Tricot L, Teicher E, Peytavin G, et al. Safety and efficacy of raltegravir in HIV-infected transplant patients cotreated with immunosuppressive drugs. *Am J Transplant* 2009; 9: 1946.
29. Teicher E, Abbara C, Duclos-Vallee JC, et al. Enfuvirtide: A safe and effective antiretroviral agent for human immunodeficiency virus-infected patients shortly after liver transplantation. *Liver Transpl* 2009; 15: 133.
30. Kowalski RJ, Post DR, Mannon RB, et al. Assessing relative risks of infection and rejection: A meta-analysis using an immune function assay. *Transplantation* 2006; 82: 663.
31. Sugawara Y, Makuuchi M, Kaneko J, et al. Correlation between optimal tacrolimus doses and the graft weight in living donor liver transplantation. *Clin Transplant* 2002; 16: 102.
32. Kishi Y, Sugawara Y, Akamatsu N, et al. Splenectomy and preemptive interferon therapy for hepatitis C patients after living-donor liver transplantation. *Clin Transplant* 2005; 19: 769.
33. Sugawara Y, Makuuchi M, Matsui Y, et al. Preemptive therapy for hepatitis C virus after living-donor liver transplantation. *Transplantation* 2004; 78: 1308.
34. Koetz AC, Delbruck R, Furtwangler A, et al. Cytomegalovirus pp65 antigen-guided preemptive therapy with ganciclovir in solid organ transplant recipients: A prospective, double-blind, placebo-controlled study. *Transplantation* 2001; 72: 1325.